SSC-102

THE RELATION OF MICROSTRUCTURE TO THE CHARPY IMPACT AND LOW-TEMPERATURE TENSILE PROPERTIES OF TWO SHIP STEELS

by

W. S. Owen, D. H. Whitmore, C. P. Sullivan,
B. L. Averbach, and Morris Cohen

MTRB LIBRARY

SHIP STRUCTURE COMMITTEE

SHIP STRUCTURE COMMITTEE

MEMBER AGENCIES:
BUREAU OF SHIPS, DEPT. OF NAVY
MILITARY SEA TRANSPORTATION SERVICE, DEPT. OF NAVY
UNITED STATES COAST GUARD, TREASURY DEPT.
MARITIME ADMINISTRATION, DEPT. OF COMMERCE
AMERICAN BUREAU OF SHIPPING

ADDRESS CORRESPONDENCE TO:
SECRETARY
SHIP STRUCTURE COMMITTEE
U. S. COAST GUARD HEADQUARTERS
WASHINGTON 25, D. C.

June 18, 1956

Dear Sir:

As part of its research program related to the improvement of hull structures of ships, the Ship Structure Committee is sponsoring at the Massachusetts Institute of Technology an investigation of the effect of metallurgical structure on brittle fracture of mild steel. Herewith is a copy of the First Progress Report of this investigation, Serial No. SSC-102, entitled "The Relation of Microstructure to the Charpy Impact and Low-Temperature Tensile Properties of Two Ship Steels" by W. S. Owen, D. H. Whitmore, C. P. Sullivan, B. L. Averbach and Morris Cohen.

The project is being conducted under the advisory guidance of the Committee on Ship Steel of the National Academy of Sciences-National Research Council.

Please address any comment concerning this report to the Secretary, Ship Structure Committee.

This report is being distributed to those individuals and agencies associated with and interested in the work of the Ship Structure Committee.

Yours sincerely,

K. K. Cowart

K. K. COWART
Rear Admiral, U. S. Coast Guard
Chairman, Ship Structure Committee

Serial No. SSC-102

First Progress Report
of
Project SR-136

to the

SHIP STRUCTURE COMMITTEE

on

THE RELATION OF MICROSTRUCTURE TO THE CHARPY IMPACT AND LOW-TEMPERATURE TENSILE PROPERTIES OF TWO SHIP STEELS

by

W. S. Owen, D. H. Whitmore, C. P. Sullivan,
B. L. Averbach and Morris Cohen

Massachusetts Institute of Technology
Cambridge, Massachusetts

under

Department of the Navy
Bureau of Ships Contract NObs-65918
BuShips Index No. NS-011-078

transmitted through

Committee on Ship Steel
Division of Engineering and Industrial Research
National Academy of Sciences-National Research Council

under

Department of the Navy
Bureau of Ships Contract NObs-72046
BuShips Index No. NS-731-036

Washington, D. C.
National Academy of Sciences-National Research Council

June 18, 1956

TABLE OF CONTENTS

	Page
List of Figures	ii
List of Tables	iv
Abstract	1
Acknowledgments	3
General Introduction	4
Part I: The Morphology of Fracture	6
Introduction	6
Experimental Methods	6
Results and Discussion	7
Conclusions	15
Part II: The Relation of Microstructure to the V-Notch Charpy Transition Temperature	18
Introduction	18
Experimental Methods	21
Results	28
Discussion of Results	48
Conclusions	53
Part III: The Tensile Properties at -195°C	55
Introduction	55
Results	59
Discussion of Results	64
Conclusions	68
General Summary	71
References	74

LIST OF FIGURES

No.	Title	Page
I.1	Wavy Slip in B Steel "As-Received".	8
I.2	Microslip in B Steel "As-Received".	8
I.3	Cross Slip in B Steel "As-Received"	8
I.4	Forked Slip in E Steel "As Received".	8
I.5	Cleavage at Twin Interface in B Steel Annealed 1250°C.	11
I.6	Cracks in E Steel "As-Received"	14
I.7	Cracks in E Steel "As-Received"	14
II.1	V-Notch Charpy Transition Curve Showing a Typical Amount of Scatter in the Experimental Data. . .	23
II.2	Microstructures of B Steel Furnace-Cooled from Indicated Austenitizing Temperatures.	29
II.3	Microstructures of E Steel Furnace-Cooled from Indicated Austenitizing Temperatures.	30
II.4	Microstructures of B Steel Air-Cooled from Indicated Temperatures.	31
II.5	Microstructures of E Steel Air-Cooled from Indicated Austenitizing Temperatures.	32
II.6	Variation of the Austenitic Grain Size with Austenitizing Temperature	33
II.7	Variation of Average Ferrite Grain Size with Austenitizing Temperature for the Furnace and Air-Cooled Series	33
II.8	Variation of the Mean Ferrite Path (α_1) with Austenitizing Temperature for the Furnace and Air-Cooled Series	34
II.9	Variation of the Mean Ferrite Path (α_2) with Austenitizing Temperature for the Furnace and Air-Cooled Series	35

No.	Title	Page
II.10	Variation of Average Pearlite Linear Intercept with Austenitizing Temperature.	35
II.11	Relationship between the Degree of Banding on Transverse Sections and the Austenitizing Temperature for the Furnace-Cooled Series.	40
II.12	Effect of Austenitizing Temperature on the Charpy Transition Temperature for the Furnace and Air-Cooled Series	41
II.13	Relationship between Ferrite Grain Size and Charpy Transition Temperature for the Furnace-Cooled Series	44
II.14	Relationship between the Mean Ferrite Path, α_1, and the Charpy Transition Temperature for the Furnace-Cooled Series	44
II.15	Relationship between the Mean Ferrite Path, α_2, and the Charpy Transition Temperature for the Furnace-Cooled Series	45
II.16	Relationship between the Pearlite Intercept, β, and the Charpy Transition Temperature for the Furnace-Cooled Series	45
II.17	Relationship of Charpy Transition Temperature to the Degree of Banding for the Furnace-Cooled Series.	47
II.18	Relationship between the Mean Ferrite Path, α_1, and Charpy Transition Temperature	49
III.1A	Yield Stress and Fracture Stress at -195°C as a Function of Average Ferrite Grain Diameter for B Steel	61
III.1B	Yield Stress and Fracture Stress at -195°C as a Function of Average Ferrite Grain Diameter for E Steel	61
III.2	Elongation to Fracture at -195°C.	62
III.3	Reduction in Area at -195°C	63

LIST OF TABLES

No.	Title	Page
I.1	Chemical Composition and Engineering Properties of Steels	17
II.1	Comparison of Grain Size Determinations by Different Methods	20
II.2	Means and Standard Deviations of Microstructural Parameters and Charpy Transition Temperatures	36
II.3	Comparison of the Transition Temperature in Air- and Furnace-Cooled Specimens	52

THE RELATION OF MICROSTRUCTURE TO THE CHARPY IMPACT AND LOW-TEMPERATURE TENSILE PROPERTIES OF TWO SHIP STEELS

ABSTRACT

This report describes the influence of the microstructural features on the brittle behavior of two ship plates, one a semi-killed steel (ABS Class B) and the other a rimming steel (project steel E). The ferrite-pearlite aggregates were varied systematically by means of annealing and normalizing treatments, and correlations were obtained between the brittle behavior and several accurately measured microstructural parameters. Part I is concerned with observations on polished specimens after deformation in tension and slow-bend tests at -195° C, as well as at room temperature, to assess the role of twinning and to study the morphology of slip and brittle fracture. Part II describes the quantitative influence of microstructural variables on the Charpy V-notch transition temperature. Part III reports on measurements of deformation prior to brittle fracture in tension specimens at -195° C and considers the effect of the microstructure on the tensile properties in the brittle range.

The metallographic observations on polished specimens (Part I) show that slip in the ferrite always precedes brittle fracture in these tests. Furthermore, the slip at -195° C appears to be as complex as that at room temperature; deformation of the pearlite was not found. Although prefracture twins were noted in coarse-grained specimens, it is concluded that twinning is not a

prerequisite for fracture; nor do grain boundary effects or non-metallic inclusions influence the morphology of fracture.

In Part II the Charpy V-notch transition temperature (chosen at the 10 ft-lb level) is shown to increase with the ferrite grain size in the annealed condition, and the ABS Class B steel is consistently better in this respect than the rimming steel. The transition temperature can be correlated with microstructual variables only when the nature of the steel and cooling rate from the austenitizing temperatures are defined. In the normalized condition, the variations in transition temperature could not be explained in terms of any metallographic parameter. It is evident that some submicrostructural feature is of overriding importance.

The extent of the prefracture deformation in tension at -195° C was studied as a function of heat treatment (Part III). Fracture always occurred after some gross yielding. There appears to be no significant correlation between the brittle fracture stress at -195° C and the Charpy transition temperature. There is a similarity, however, between the general trends of the prefracture ductility and the Charpy transition temperatures with heat treatment.

Both the Charpy and tensile tests provide clear evidence that the conventional metallographic parameters (as measured by the optical microscope) are inadequate to account for the brittle behavior of ship steels. This leads to the conclusion that

submicroscopic variables are very important in the brittle fracture phenomenon.

ACKNOWLEDGMENTS

Valuable assistance with the laboratory work was provided by R. C. Whittemore, E. Howell and E. Keplin. Miriam Yoffa and Leonard Sudenfield contributed some of the microscopic data.

GENERAL INTRODUCTION

The major objective in this program is to obtain an understanding of the relationship between the structure of ship plate steel and the tendency toward brittle behavior. By "structure" is meant both the gross microstructural features and those on a finer scale. Before attempting to study the more subtle effects, however, it was considered necessary to review and supplement the existing information concerning the role of structure which can be measured by the optical microscope. Almost all of the earlier work of this nature has been concerned with laboratory melts or steels specially selected to accentuate some structural feature. The present investigation has been confined to ship steels. To provide data which can be analyzed in terms of various structural parameters, the necessary range of microstructure has been obtained by heat treatment rather than by changes in composition. Work on steels containing essentially no free carbide (0.02% carbon) has shown that, for a given grain size, very different mechanical behavior can result depending upon whether the grain size has been produced by a supercritical heat treatment or recrystallization below the A_3 temperature[1,2]. In the ship steels investigated here, subcritical recrystallization of the ferrite could not be achieved without a drastic change in the distribution and morphology of the cementite. Consequently, all the selected heat treatments involved cooling through the critical range.

Two steels were used; both were supplied in the form of hot-rolled plates, approximately 72 in. by 108 in. by 3/4 in., of

commercial open-hearth heats manufactured under carefully observed conditions. One was a "project steel" of the rimming type, made between 1944 and 1946[3]. This steel, project steel E, was selected because of its marked brittle behavior. The other was an American Bureau of Shipping (ABS) Class B semikilled hull steel manufactured to conform to the 1948 revised ABS specification for ship plate over 1/2 in. thick. The chemical composition and room temperature mechanical properties of both steels, referred to as B and E, are given in Table I.1 at the end of Part I.

Work of this kind would be facilitated greatly if an acceptable theory of the micromechanism of fracture existed. It would then be possible to deduce which of the structural features are important in the initiation and propagation of fracture. However, such a theory is not available. Consequently, observations on both prepolished and sectioned specimens were made to assess the relation of gross structural features to brittle fracture. This aspect of the problem is discussed in Part I.

The most widely accepted measure of the susceptibility to brittle fracture is the V-notch Charpy transition temperature. This was examined quantitatively in terms of the microstructural parameters which were judged to be of greatest importance. The findings are reported in Part II.

In Part III the results of experiments designed to show the effect of microstructure on the tensile properties at -195° C are described.

PART I

THE MORPHOLOGY OF FRACTURE

INTRODUCTION

In the past a variety of microscopic phenomena have been suggested as being the determining factors in brittle fracture. Slip, twinning and cleavage in ferrite grains; grain boundaries; grain boundary carbides; pearlite; pearlite-ferrite interfaces; and nonmetallic inclusions have all been involved in one or other of the proposed micromechanisms. The object of this part of the work was to decide which, if any, of the many proposed micromechanisms is likely to be relevant to ship steel and consequently to decide which microstructural features should be included in the quantitative work.

EXPERIMENTAL METHODS

The observations were confined to B and E steel in the "as-received" condition, annealed (1250° C) to a large grain size, or air cooled (950° C) to give a small grain size. Surfaces prepared by electropolishing were examined after various amounts of deformation culminating in fracture. The tests were carried out at -195° C. The specimens were either flat tensile specimens or slowly bent unnotched and V-notch Charpy bars. After examination of the surfaces, the specimens were sectioned and metallographically prepared for further study.

For purposes of comparison with ductile behavior, a number of room temperature tests were also carried out.

RESULTS AND DISCUSSION

Slip in ferrite. At room temperature slip in ferrite occurs on {110}, {112} and {123} planes in <111> directions. The fact that ferrite can slip on several different planes presumably accounts for the appearance of so-called wavy slip and pencil glide. Barrett, Ansel and Mehl[4], examining silicon-ferrite, found that as the temperature is lowered, slip is restricted to fewer systems, eventually occurring only on {110}<111>. It has been suggested that this limitation creates a situation in which, in some suitably oriented grains, cleavage occurs in preference to slip. This concept has been extended to silicon-free ferrites, but its validity in such cases has not been verified experimentally.

In the ship steels the slip markings observed at -195° C were of the same type as those found in the room temperature tests. In addition to the usual wavy slip (Fig. I.1), microslip similar to that found by Paxton[5] in pure iron (Fig. I.2), cross slip (Fig. I.3) and forked slip (Fig. I.4) were observed before fracture at -195° C. The characteristics of the slip markings were not affected by the presence of a notch. The slip process did not appear to be impeded by subboundaries (veining), but a small angular deviation of a slip line was detected when it crossed one of these boundaries.

These observations suggest that there is no restriction of slip systems in hypo-eutectoidal ferrite on decreasing the

Fig. I.1 Wavy Slip in B Steel "As-Received." Unnotched Slow Bend at -195°C. X 1000

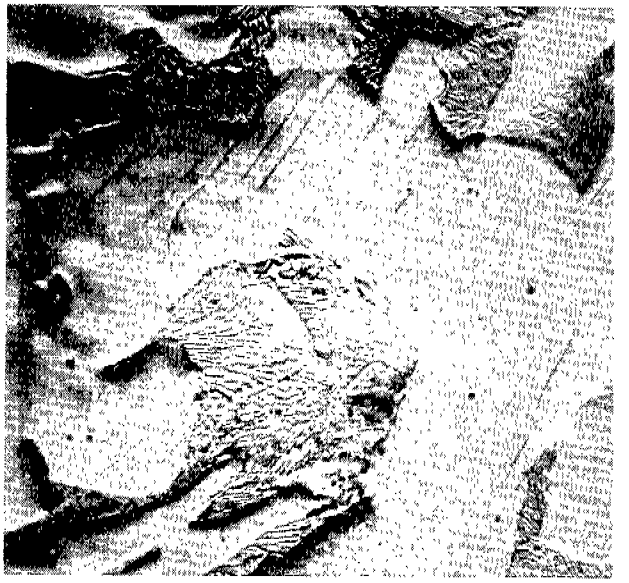

Fig. I.2 Microslip in B Steel "As-Received." Unnotched Slow Bend at -195°C. X 1000

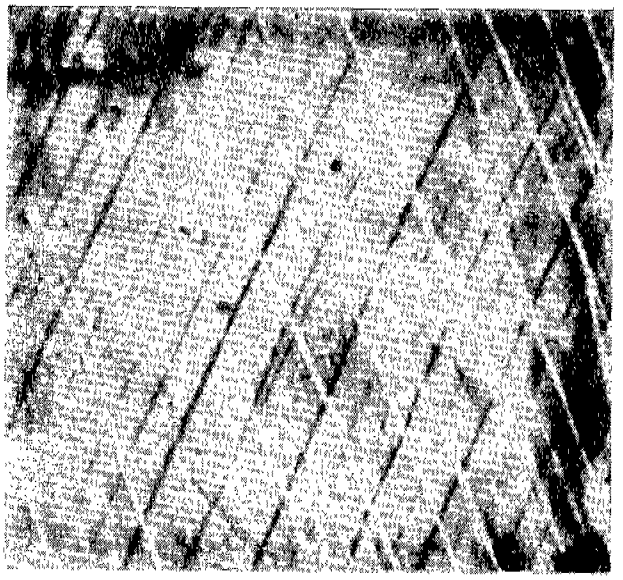

Fig. I.3 Cross Slip in B Steel "As-Received." Unnotched Slow Bend at -195°C. X 2000

Fig. I.4 Forked Slip in E Steel "As-Received." Unnotched Slow Bend at -195°C. X 1000

temperature to a level where the steel becomes brittle. However, they do demonstrate the heterogeneous nature of the deformation which leads to brittle fracture, thus supporting the suggestion of Norton, Treon, and Baldwin[6] who, by analogy with the behavior of single crystals of zinc, proposed an accommodation theory of cleavage.

Twinning in ferrite. It was early observed that mechanical twinning and brittle fracture are frequently associated[7]. The view that twinning is a prerequisite to fracture has been argued in numerous Russian papers[8--10] and by Bruckner[11,12]. However, the present majority opinion[13] appears to be that there is no essential cause-and-effect relationship. This conclusion, related to low-carbon iron, has been emphasized and substantiated by Low and Feustel[14].

In the present work on ship steel[15], it was found that external impact loading was not essential for the formation of ferrite twins, in agreement with the results of Geil and Carwile[16] on ingot iron. Before fracture, under static loading conditions, twin formation was strongly grain-size dependent. In the small grain size air-cooled specimens, no twins were observed after loading in simple tension to within a few pounds of the fracture stress. With the large grain size material, extensive twinning was noted under comparable conditions. Similar results were found in the slow bend experiments. However, after fracture of

all specimens, a band of material extending at least a few millimeters on both sides of the fracture contained numerous ferrite twins. It has been suggested by Allen[17] that these are produced by the change in distribution and direction of stress as the crack passes through. By their location relative to the fracture, the latter twins can be distinguished easily from those formed before fracture.

It is clear that fracture in ship steel may or may not be preceded by twinning, depending upon the grain size, temperature and rate of loading of the specimen. There appeared to be no essential connection between such twinning and fracture. In general, the fracture path was not affected by the presence of twins. However, a number of cases where the cracks coincided with twin interfaces were found (Fig. I.5), indicating that the fracture plane, twin interface and plane of polish included a common direction. This suggests, but does not prove, that in such cases the fracture plane is $\{112\}$. A similar observation has been made by Klier[18], Tipper and Sullivan[19], and Danko and Stout[20].

<u>Microcracking in ferrite</u>. The Griffith-Orowan[21,22] concept of critical crack size has stimulated a search for subcritical cracks in metals. Low[23] has observed subcritical cracks, of a size defined by the ferrite grain diameter, in a low-carbon steel. The evidence found in the current work to

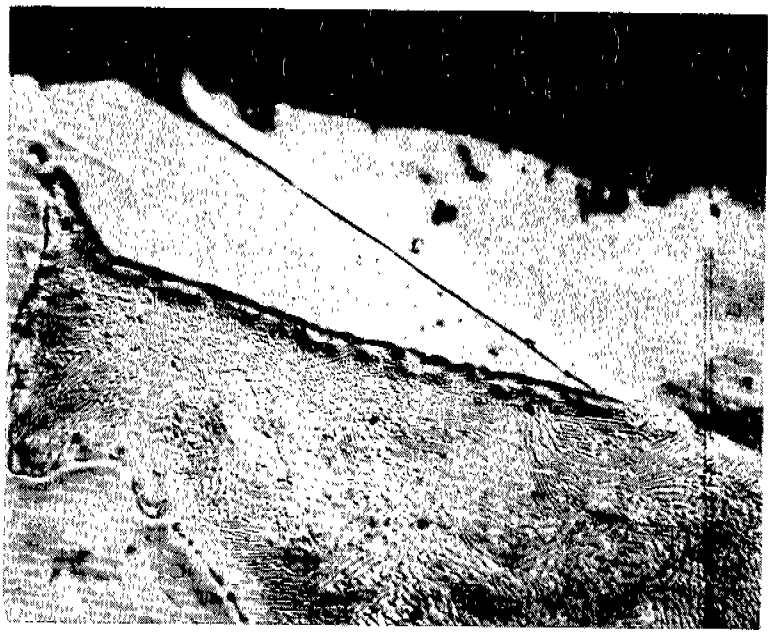

Fig. I.5 Cleavage at Twin Interface in B Steel Annealed 1250°C. Slow Bend Fracture at -195°C. X 1000

support the application of this concept to ship steel was very limited. Many hundreds of plastically strained ferrite crystals in unfractured specimens were examined. In only one instance was a subcritical crack found. Thus, it seems that, if microcrack formation precedes fracture, in almost all cases it is immediately followed by catastrophic failure. It is interesting to note that the one microcrack detected was confined by ferrite grain boundaries and was not stopped by an intersecting pearlite colony.

Baeyertz, Craig and Bumps[24] and Felbeck and Orowan[25] have postulated that microcracks are formed in the volume immediately ahead of a running crack, the main fracture being generated by some of these joining up, while others are by-passed. Some direct evidence of this mechanism has been found by Felix[26], who examined partially fractured notched impact bars. In all the fractured ship steel specimens examined here, numerous secondary cracks, many apparently unconnected with the main fracture, were detected. Danko and Stout[20] have made a study of this type of crack in 1025 steel. They observed that often a crack was blunt at one end and pointed at the other. Making the assumption that the starting point was at the blunt end, they concluded that cleavage failure was initiated at a ferrite grain boundary or a ferrite-pearlite interface. No evidence to support this contention was found in the steels examined in this investigation. Only in very few instances was there any discernible

difference in the appearance of the two ends of secondary cracks. However, in most cases at least one end was in contact with a ferrite grain boundary or a ferrite-pearlite interface (Fig. I.6).

Ferrite grain boundaries. Allen, Rees, Hopkins and Tipler[27], working with high purity iron-carbon alloys, and Matton-Sjöberg and Lindblom[28] with low carbon steels, have shown that partly intergranular fracture can occur when carbide films are located at the grain boundaries. However, such fractures were observed only when the steel exhibited some ductility. They were not formed when the specimens were tested in the brittle range. Increasing the manganese content reduced the prevalence of carbide films, but the effect of manganese on the transition temperature could not be attributed to this effect[28]. Danko and Stout[20] have produced evidence of partly intergranular fracture in 1025 steel. Their specimens were slowly cooled from above 1300° C, which could have produced extensive grain boundary carbide separation. On the other hand, Rees and Hopkins[29] earlier had drawn attention to the occurrence of partly intergranular fracture in ship plate which had not been heat treated, but it was implied[30] that the latter result was not directly connected with carbide separation.

In the "as-received" condition, the ship steels in this investigation contained little indication of grain boundary carbide films. No intergranular failure was found in specimens tested at room temperature. When tested in the brittle condition at -195° C, very rare examples of cracks partly following

Fig. I.6 Cracks in E Steel "As-Received." Notched Bar Slow Bend at -195°C. X 2000

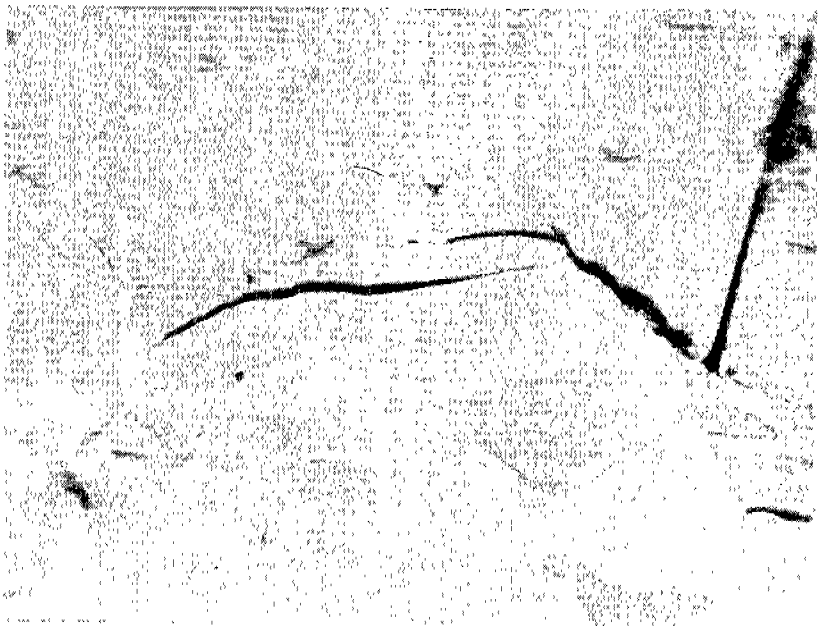

Fig. I.7 Cracks in E Steel "As-Received." Slow Bend at -195°C. X 2000

the grain boundaries were observed (Fig. I.7). These were not associated with detectable carbide films. The tendency to this type of cracking was not increased by heat treatments representing the extremes of the range used subsequently in this investigation. Thus, it was clear that intergranular failure was not a significant feature of fracture under the conditions at hand.

Other microstructural features. Nonmetallic inclusions and carbide lamellae[31] have been suggested as possible sources of cleavage. In the two ship steels investigated, there was no evidence of inclusions being associated with the initiation of brittle fracture, nor, judging by their position relative to the secondary cracks, did they influence the course of the crack.

Compared with the ferrite, the pearlite did not appear to have suffered any appreciable deformation in the specimens which broke in a brittle manner. It was frequently observed that one end of a secondary crack was situated in a pearlite area (Fig. I.6). Generally, in these cases the pearlite lamellae made a large angle with the direction of the crack. Following Danko and Stout[20], it seems more reasonable to suppose that this situation demonstrates the ability of suitably oriented pearlite to impede rather than to initiate a brittle crack.

CONCLUSIONS

1. At -195° C, in tension or slow-bend (notched or unnotched) test, brittle fracture of the two ship steels studied is preceded by

some deformation. Predominantly, this takes the form of slip in the ferrite crystals. Pearlite deformation is not apparent.

2. The metallographic appearance of the slip at -195° C is the same as that observed at room temperature. The extent of the slip varies appreciably from grain to grain and frequently is heterogeneous within a single grain.
3. Concerning the existence and nature of subcritical Griffith cracks, the present experiments are inconclusive.
4. In ship steel tested at -195° C, twinning, grain boundary effects, and nonmetallic inclusions appear to be of negligible importance in the brittle fracture process.

TABLE I.1

CHEMICAL COMPOSITION AND ENGINEERING PROPERTIES OF STEELS

Weight Percentage

Designation	C	Mn	P	S	Si	Cu	Ni	Cr	V	Mo	Al	Sn	As	O	H	N
ABS Class B Steel	0.16	0.69	0.014	0.028	0.022	0.028	0.015	0.01	0.005	0.01	0.027	0.010	0.001	0.017	0.0001	0.0023
Project Steel E	0.22	0.36	0.016	0.031	0.002	0.17	0.13	0.08	0.005	0.25	0.009	0.012	0.001	0.006	0.0001	0.0021

Room Temperature Mechanical Properties

	Yield Point		Elastic Limit	Fracture Stress	Elongation	Reduction in Area
	Upper	Lower				
ABS Class B Steel	33,000 psi	31,000 psi	22,000 psi	39,800 psi	30.9%	58.2%
Project Steel E	34,000 psi	33,000 psi	20,000 psi	55,400 psi	27.1%	55.0%

PART II

THE RELATION OF MICROSTRUCTURE TO THE V-NOTCH CHARPY TRANSITION TEMPERATURE

INTRODUCTION

The observations reported in Part I indicate that the ferrite phase is the important consideration in the low-temperature yield and brittle fracture phenomena. In the two ship steels examined, the fracture process does not appear to be related to intergranular failure or to the size and distribution of the nonmetallic inclusions. Thus, it was unnecessary to consider them in the attempt to correlate microstructure with fracture behavior. Measurements of ferrite interfacial area and inclusion distribution were omitted in the subsequent analysis.

It is well known that ferrite grain size exerts a marked influence on the ductile-brittle transition as established by notched-bar tests[32--39]. Recent work at Battelle has demonstrated that a linear relationship exists between ferrite grain size and Charpy keyhole-notch transition temperature (at the 12 or 20 ft-lb level) for a low carbon steel and several semikilled mild steels. A similar result has been obtained by Vanderbeck[40].

Although the general influence of ferrite grain size has been observed many times, there is a paucity of quantitative data relating to this effect. The matter is complicated by the fact that a number of different methods of measuring grain size have been employed. There are serious differences between the measurements by different laboratories on the same specimen. In some cases

there is not even agreement about the type of grain being measured. This unsatisfactory situation was pointed out by Barrett and Mahin[41] in a recent review of ship steel research. In Table II.1 the results are given of grain size measurements by a number of different methods on the same set of samples supplied by the National Bureau of Standards. The agreement between the U. S. Steel Corporation method and that used in the present investigation is satisfactory, but the other methods give scattered data.

However, it is clear that quantitative differences among the investigators are not solely a result of differences in experimental technique. It has been demonstrated by the Battelle[36--39] work that the quantitative effect of grain size on transition temperature is strongly dependent on the composition of the steel, the deoxidation practice, and the finishing temperature. It is recognized also that, if the steel is reheated, the rate of cooling from the austenitizing temperature is important[32]. Hence, at least part of the effects of these variables must be looked for in structural features other than ferrite grain size.

One other aspect of the microstructure has received detailed consideration--the carbide morphology. Some recent investigations[42--44] have been directed at the relationship between pearlite spacing and transition temperature. Although there is some disagreement about the sign of the change in Charpy transition with increasing pearlite spacing, it is evident that within the range of composition covered by ship steel the effect is negligible.

TABLE II.1

COMPARISON OF GRAIN SIZE DETERMINATIONS BY DIFFERENT METHODS

Method* \ Specimen No.	LA 18	HA 12	BV1	CV 19	HC 34	BV 37
	A.S.T.M. Numbers					
1	4.5	5.0	4.9	5.7	6.2	7.4
2	6.6	6.5	6.5	7.0	7.0	7.8
3	7.6	7.3	6.6	7.2	7.3	8.3
4	6.5	6.5	6.0	7.0	7.0	8.0
5	7.0	7.5	6.5	-	-	8.4
6	7.8	7.65	6.45	7.65	7.35	8.45
7	-	7.44	6.84	6.98	7.67	8.36

*

1. Ground glass screen image compared with ASTM Charts. Average of ratings of 4 to 6 observers. NBS
2. Intercept count, (X100) - Average of 3 observers. NBS
3. Grain count, (X500) - Average of 3 observers. NBS
4. Photomicrographs (X100) compared with ASTM Charts (U. S. Steel Corp.)
5. Grain size comparator - Average 3 observers. U. S. Steel Laboratory
6. Grain size comparator - Average 2 observers. NBS
7. Lineal analysis - MIT

The influence of carbide precipitation produced by subcritical heat treatments has been investigated by Brick[2,45--47] in high purity iron-carbon alloys and by Joseffson[1] in commercial grades of low-carbon steel. While in the very low-carbon alloys they showed spectacular changes in transition temperature with changes in extent and distribution of precipitated carbide, these effects were not detectable when the carbon content was greater than about 0.05%. The role of precipitated carbides and nitrides in ship steel requires investigation and will be considered in the future program dealing with submicroscopic phenomena.

EXPERIMENTAL METHODS

Charpy blanks of both B and E steel were austenitized at temperatures in the range 850°--1300° C. In one series of experiments the austenitizing was followed by air cooling (150° C per min) and in another by cooling in the furnace (1.6° C per min). All heat treatments were performed on rough machined specimens in a purified nitrogen atmosphere.

The finished test specimen was a longitudinal Charpy bar with a standard Izod V-notch cut perpendicularly to the rolling surface of the plate. The bars were dimensionally checked before testing, and all the precautions recognized to be necessary in Charpy testing at various temperatures were observed meticulously.

Transition curves were determined using 20 to 24 specimens, generally at eight or ten fixed temperatures in the range -50° C

to 200° C. A typical curve is shown in Fig. II.1. If a 10 ft-lb energy level is chosen as the criterion, the scatter in the data is such that this average curve gives only an approximate value for the transition temperature. To obtain a more precise value, it was necessary to resort to a statistical procedure.

The most direct and informative of the statistical methods that have been used for determining transition temperatures in the Charpy test is the Probit method[48--50]. Applied to the present work this would require about 20 specimens at each of six testing temperatures, spaced in, say, 5° C intervals near the transition temperature. Since this number of specimens was prohibitively large, it was decided to use the "staircase" method. This technique was developed in research on explosives. No previous reference has been found to its use in impact testing, although it has been applied to the determination of endurance limits[51,52].

The approximate transition temperature was determined from the usual transition curve and was adopted as the initial testing temperature, T_o. The possible testing temperatures (T_1, T_2, T_3 ... above T_o, and T_{-1}, T_{-2}, T_{-3}... below T_o) were also fixed in advance (see page 24). If the first specimen (tested at T_o) absorbed more than 10 ft-lbs it was considered to be ductile, and the second specimen was tested at T_{-1}. However, if the energy absorbed was less than or equal to 10 ft-lbs, the specimen was classified as brittle; and the second specimen was tested at T_1. Succeeding

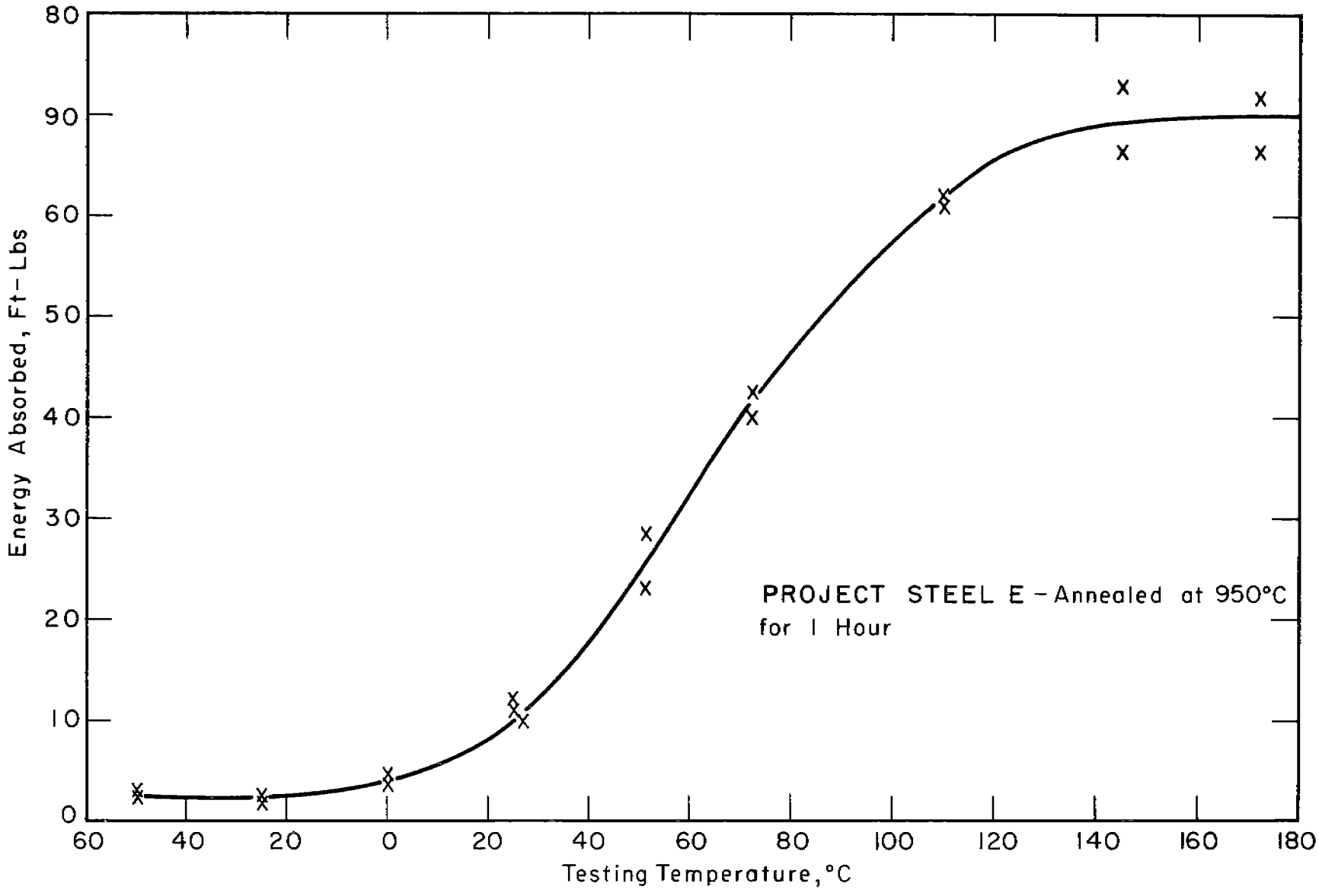

FIG. II.1 - V-NOTCH CHARPY TRANSITION CURVE SHOWING A TYPICAL AMOUNT OF SCATTER IN THE EXPERIMENTAL DATA.

specimens were tested at the temperature just below or above that of the previous test depending upon whether or not the energy absorbed in that test was above or below 10 ft-lb. Suppose the results of such an experiment were as follows:

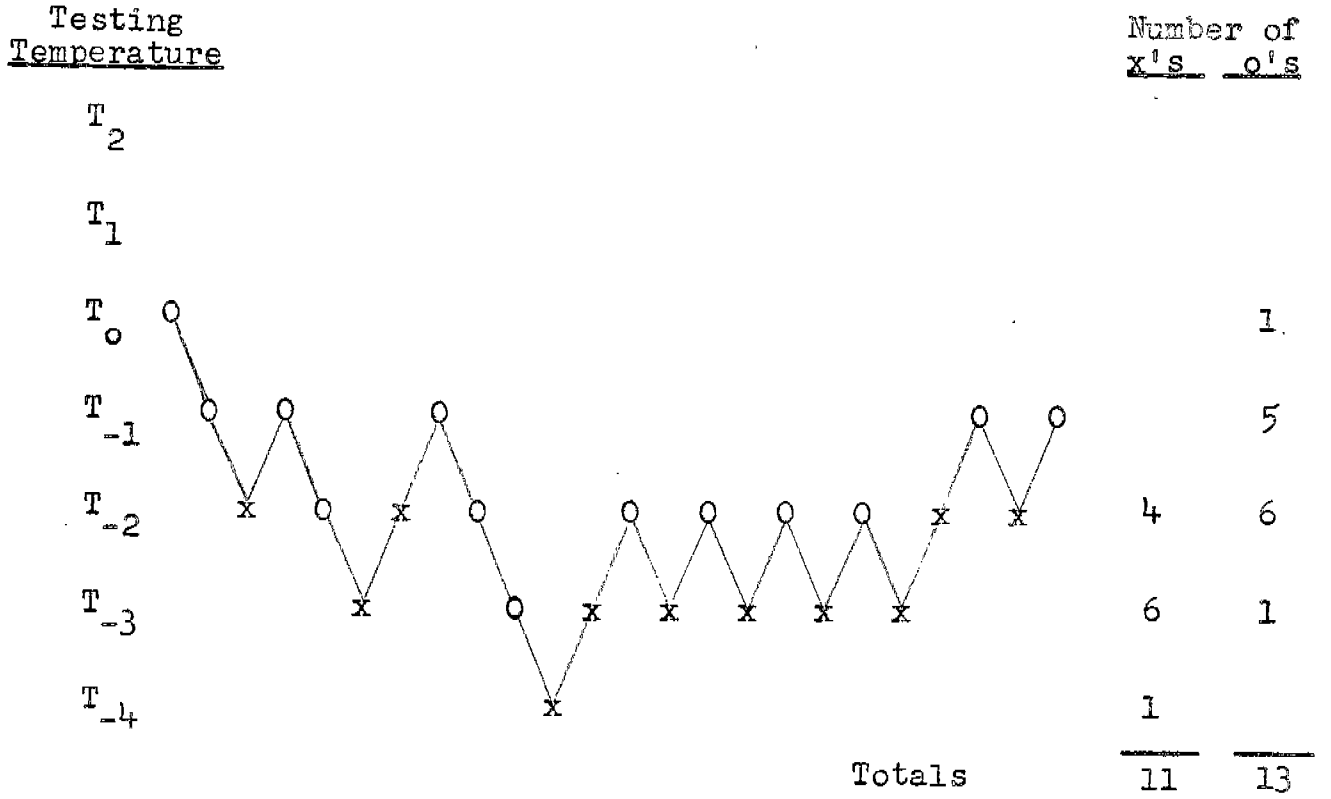

The x's represent brittle and the o's non-brittle specimens. The first specimen was non-brittle, and so the second test was performed at the next lower temperature level, T_{-1}. Since this was also non-brittle, the third test was made at a temperature level immediately below that of the second. The third specimen was brittle, and hence the fourth test was carried out at the next higher temperature level, and so on.

The primary advantage of this procedure is that it automatically concentrates testing near the mean transition temperature. Consequently, for a given accuracy the staircase method requires fewer tests than the Probit method. The saving in specimens is usually greater than 40 per cent. Furthermore, the method allows approximate confidence intervals for the mean and standard deviation to be calculated.

The technique can be applied only when certain conditions are satisfied: (1) the variate under analysis (10 ft-lb transition temperature) should be normally distributed; (2) the sample size must be sufficiently large (at least 24 Charpy tests); (3) the standard deviation of the variate must be estimated in advance and be approximately equal to the selected interval between testing temperatures. The last condition is well satisfied if the interval chosen is between one-half and twice the standard deviation of the transition temperature. Previous work[50,53] on the statistical analysis of Charpy test data indicates that the standard deviation of the transition temperature is about 3--5° C, and hence a testing temperature interval of 5° C was adopted here. The analysis of the data is discussed in detail elsewhere[54].

All of the quantitative metallography was performed on a Hurlbut counter[55] by two observers who were chosen from among six on the basis of a Latin square test which showed that their results agreed closely and were near the average. The analysis

of the data[54] was performed in most cases by the M.I.T. Statistical Services using I.B.M. computing machines. The following measurements were obtained:

L_F--total ferrite intercept in millimeters

L_P--total pearlite intercept in millimeters

N_F--number of ferrite grains traversed

N_P--number of pearlite "patches" traversed

From these the appropriate microstructural parameters were computed.

<u>The ferrite grain size</u>, n_v--<u>the number of ferrite grains per unit volume of ferrite</u>. Assuming the ferrite grains are Kelvin equi-edged tetrakeidahedrons which completely fill space[56,57],

$$n_v = \frac{0.4263 N_F^3}{L_F^3}. \qquad (1)$$

Values of n_v (grains per mm^3) are readily converted to ASTM grain size numbers through the tabulation given by Rutherford et al.[57]. It should be noted that n_v is the number of ferrite grains per unit volume of <u>ferrite</u>. If required, this can be converted to the number of grains per unit volume of steel by multiplying by the volume fraction of ferrite in the steel.

<u>The volume fraction of ferrite</u>, V_F, <u>and Pearlite</u>, V_P.

$$V_F = \frac{L_F}{L_F + L_P} \tag{2}$$

$$V_P = \frac{L_P}{L_F + L_P}. \tag{3}$$

<u>The mean ferrite path</u>, α_1 <u>and</u> α_2. The mean ferrite path was expressed in two ways. α_1 was defined as the mean distance between boundaries in the ferrite as intercepted along a straight line by both ferrite-ferrite and ferrite-pearlite boundaries:

$$\alpha_1 = \frac{L_F}{N_F}. \tag{4}$$

α_1 is directly related to the mean grain diameter (d)[73].

$$d = 1.65\alpha_1. \tag{4a}$$

α_2 was defined as the mean distance in the ferrite as intercepted along a straight line by ferrite-pearlite boundaries (leaving out the ferrite-ferrite boundaries):

$$\alpha_2 = \frac{L_F}{N_P}. \tag{5}$$

<u>The pearlite patch size</u>, β. The patches assumed various irregular shapes. Consequently, the average pearlite linear intercept, β, was considered to be the most appropriate parameter:

$$\beta = \frac{L_P}{N_P}. \tag{6}$$

RESULTS

Effect of heat treatment on microstructure and impact behavior. It was necessary to change the scale of the microstructural features while maintaining the morphology comparable with that commonly found in ship steel. This was done by austenitizing at temperatures between A_3 and the "burning temperature" followed by furnace or air cooling.

Table II.2 summarizes all of the microstructural parameter data and Charpy transition temperatures for the two steels after various treatments as well as in the "as-received" condition.

Variation of microstructure with heat treatment. Photomicrographs of representative specimens are shown in Figs. II.2, II.3, II.4 and II.5. The microstructural parameters, obtained on transverse sections, are plotted as a function of austenitizing temperature in Figs. II.6, II.7, II.8, II.9 and II.10. The values are the average of traverses made both parallel and perpendicular to the rolling surface.

In the furnace-cooled series, the austenite grain size and ferrite grain size increased with austenitizing temperature (Figs. II.6 and II.7). A ferrite grain size curve of similar shape has been observed at Battelle[39]. The mean ferrite paths (α_1 and α_2)(Fig. II.8) showed a corresponding increase. After furnace cooling from any selected temperature below 1050° C, the steel with the greater tendency to notch brittleness (the E steel) had the finer structure (Figs. II.7 and II.8). Above this temperature

(a) 850°C

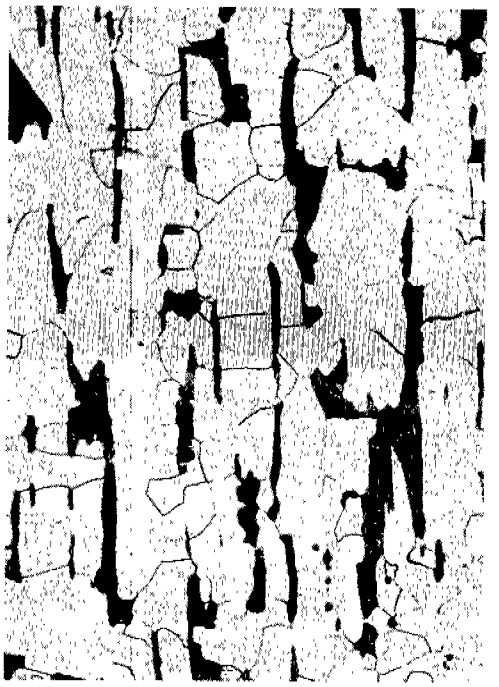

(b) 1050°C

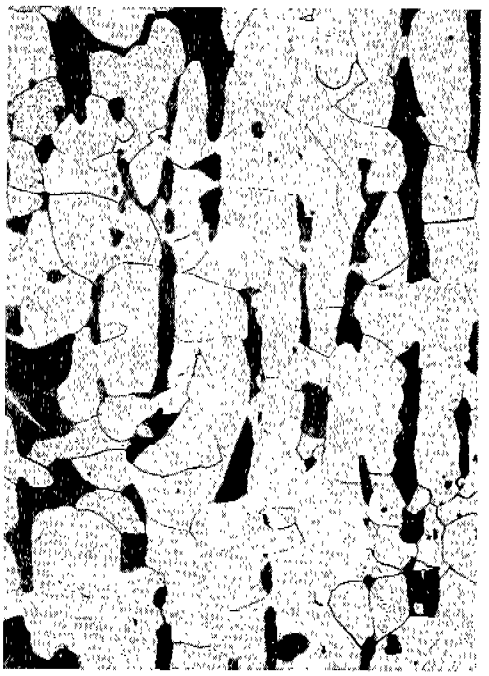

(c) 1150°C

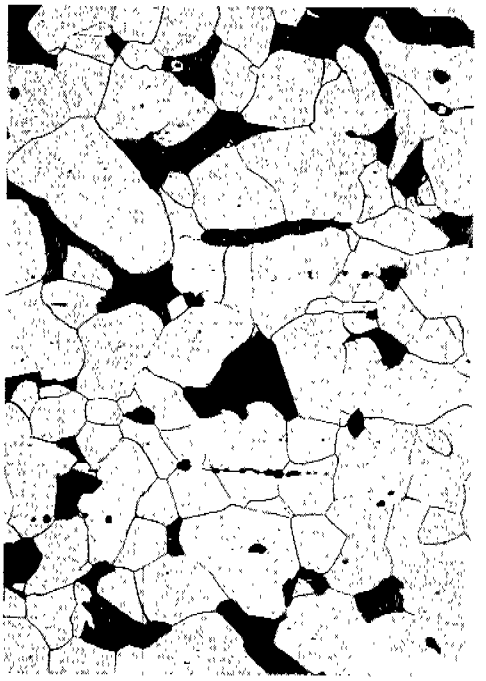

(d) 1250°C

Fig. II.2 Microstructures of B Steel Furnace-Cooled from Indicated Austenitizing Temperatures. Nital Etch--Transverse Section. X 100

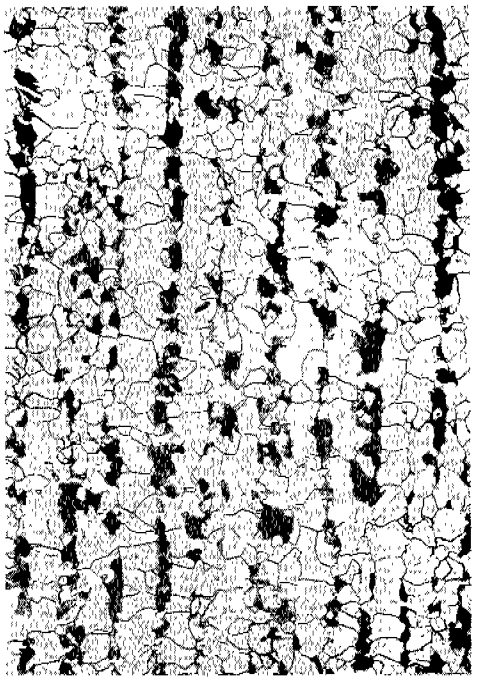

(a) 850°C

(b) 1050°C

(c) 1150°C

(d) 1250°C

Fig. II.3 Microstructures of E Steel Furnace-Cooled from Indicated Austenitizing Temperatures. Nital Etch--Transverse Sections. X 100

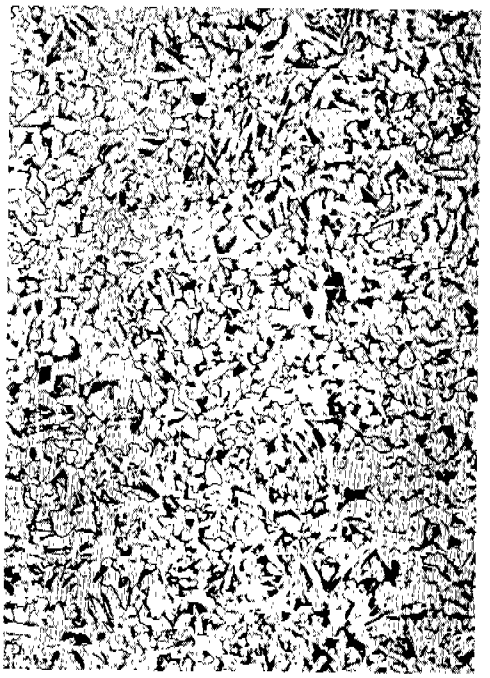

(a) 850°C

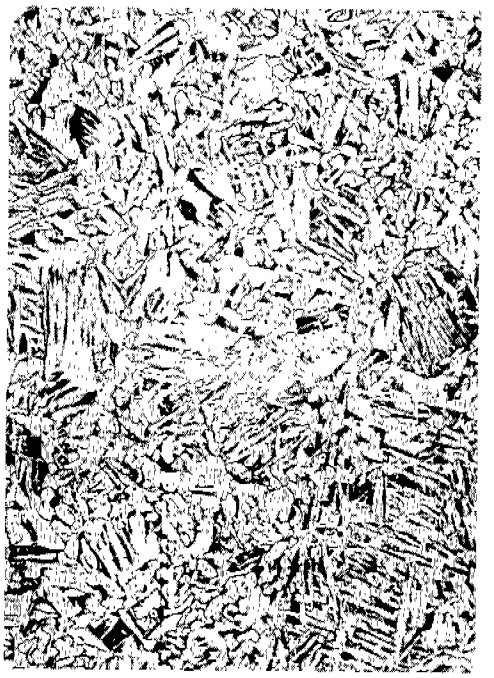

(b) 950°C

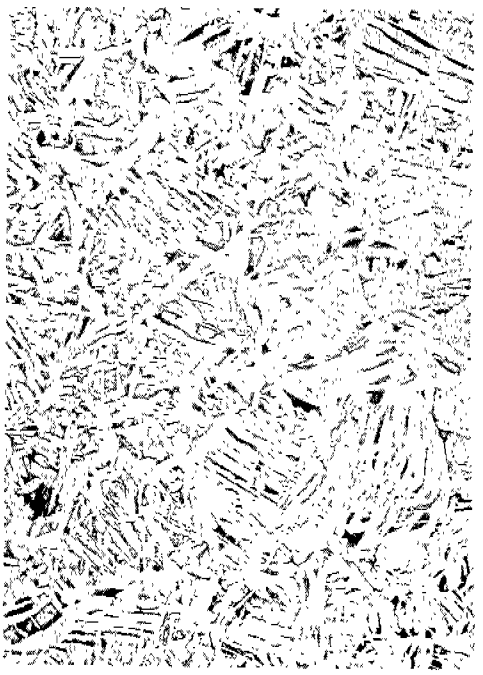

(c) 1050°C

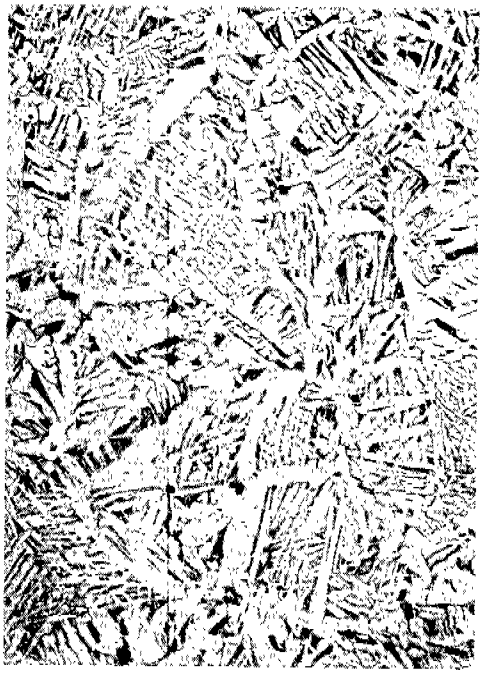

(d) 1250°C

Fig. II.4 Microstructures of B Steel Air-Cooled from Indicated Temperatures. Nital Etch--Transverse Section. X 100

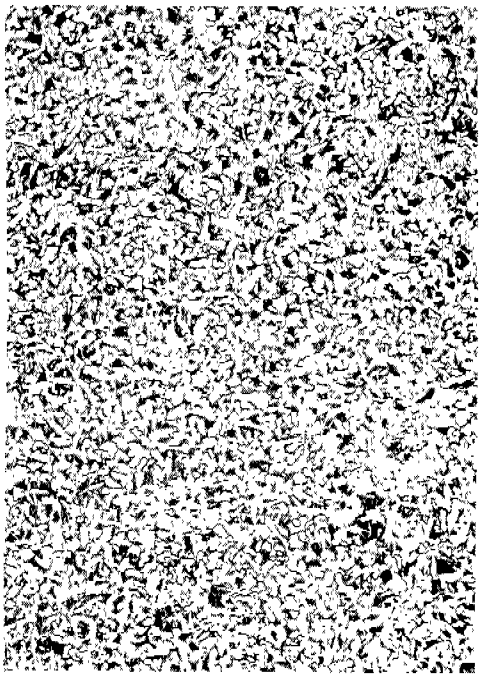

(a) 850°C

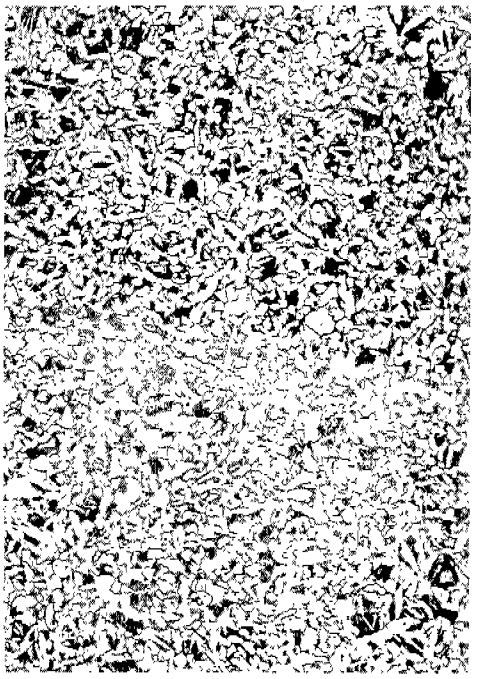

(b) 950°C

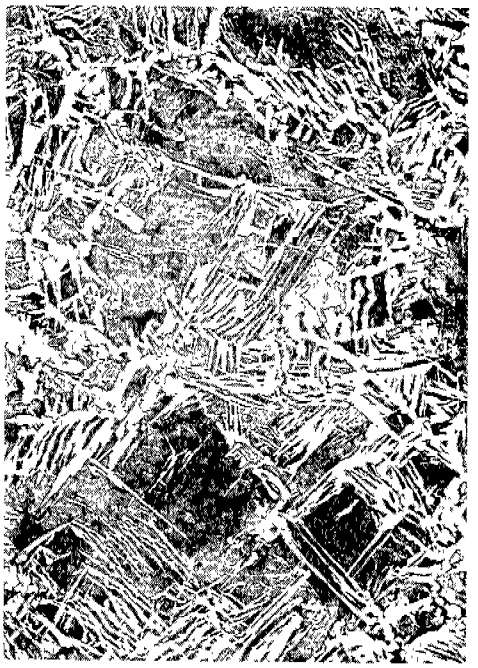

(c) 1050°C

(d) 1250°C

Fig. II.5 Microstructures of E Steel Air-Cooled from Indicated Austenitizing Temperatures. Nital Etch--Transverse Section. X 100

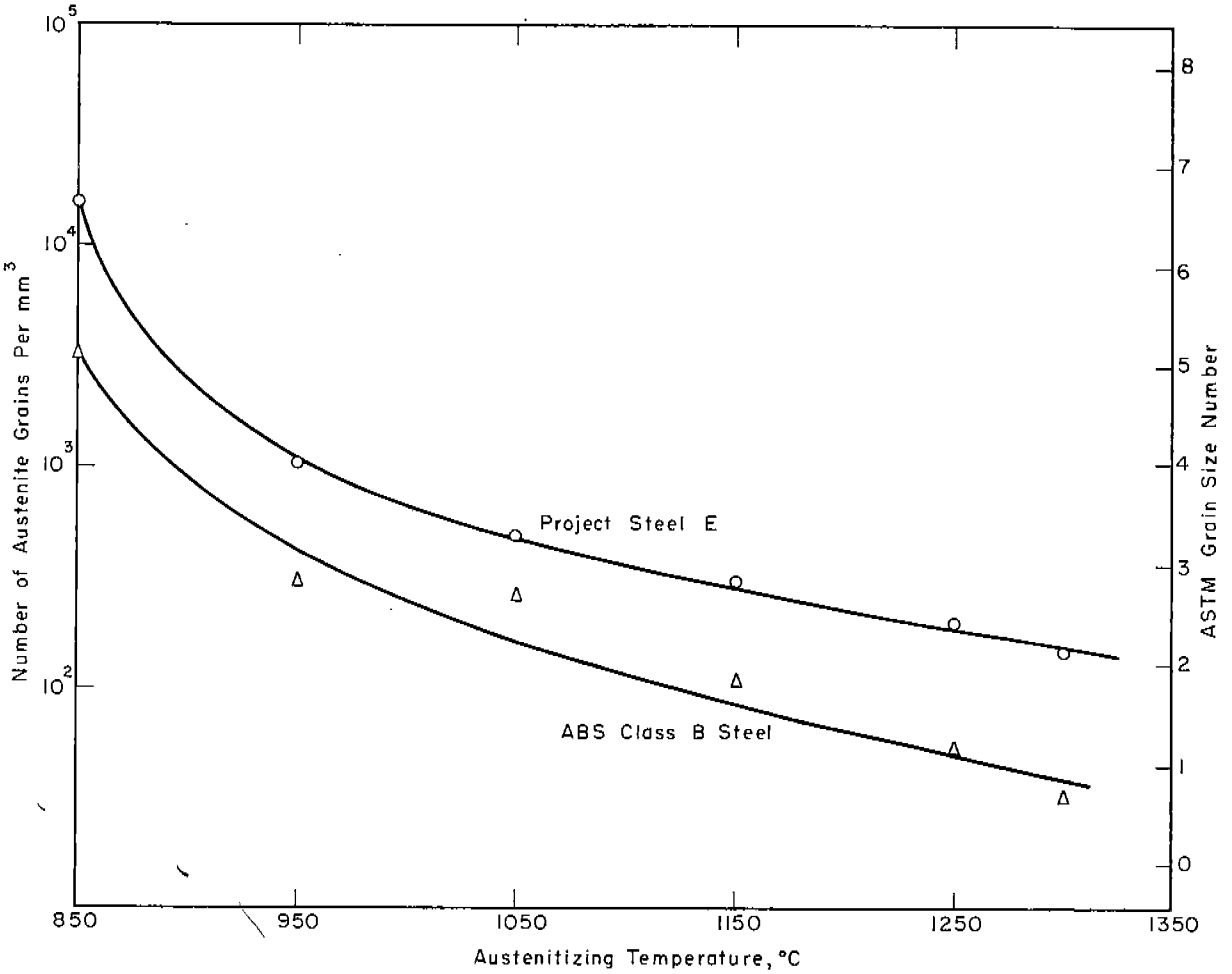

FIG.II.6- VARIATION OF THE AUSTENITIC GRAIN SIZE WITH AUSTENITIZING TEMPERATURE.

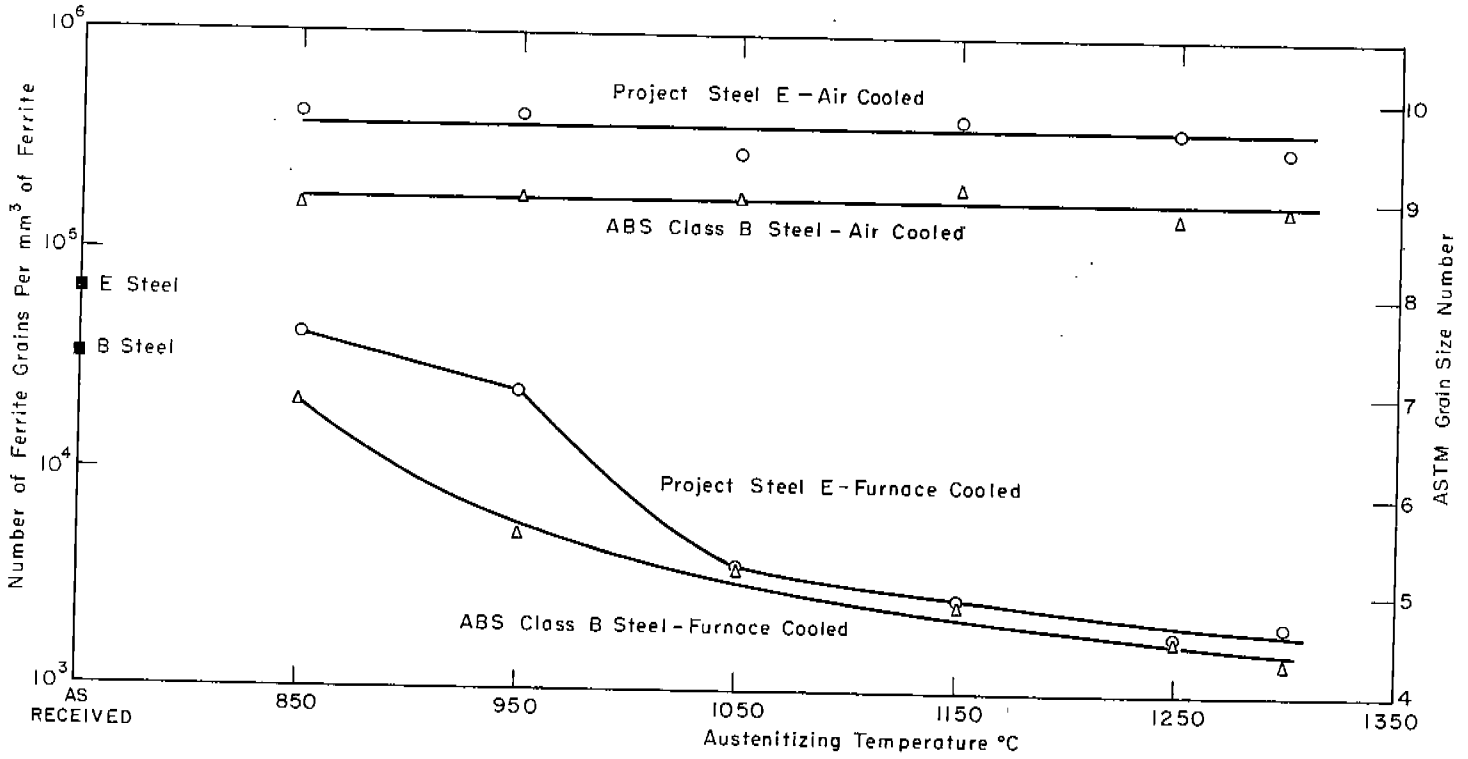

FIG. II.7- VARIATION OF AVERAGE FERRITE GRAIN SIZE WITH AUSTENITIZING TEMPERATURE FOR THE FURNACE AND AIR-COOLED SERIES.

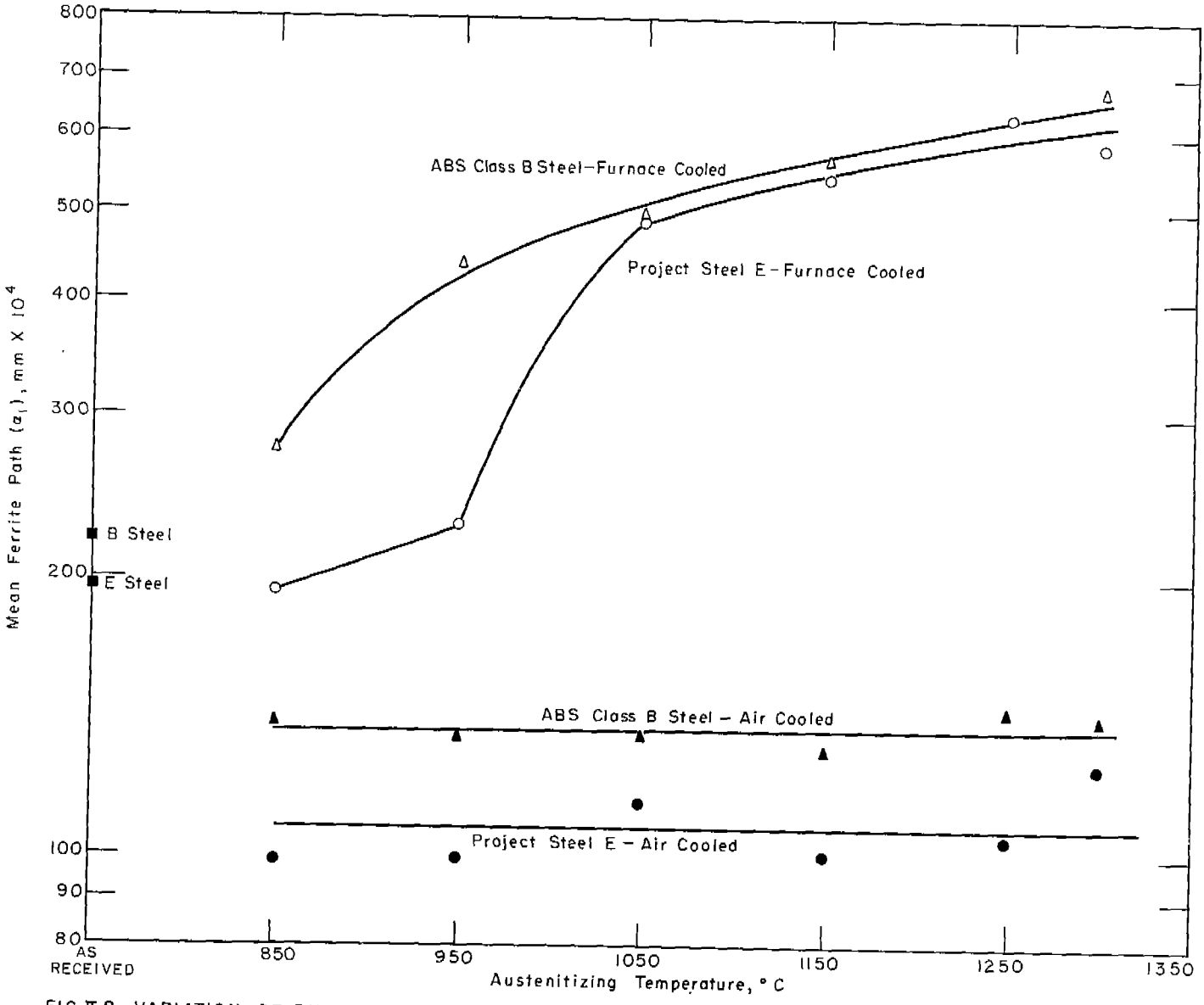

FIG. II.8 - VARIATION OF THE MEAN FERRITE PATH (α_1) WITH AUSTENITIZING TEMPERATURE FOR THE FURNACE AND AIR-COOLED SERIES.

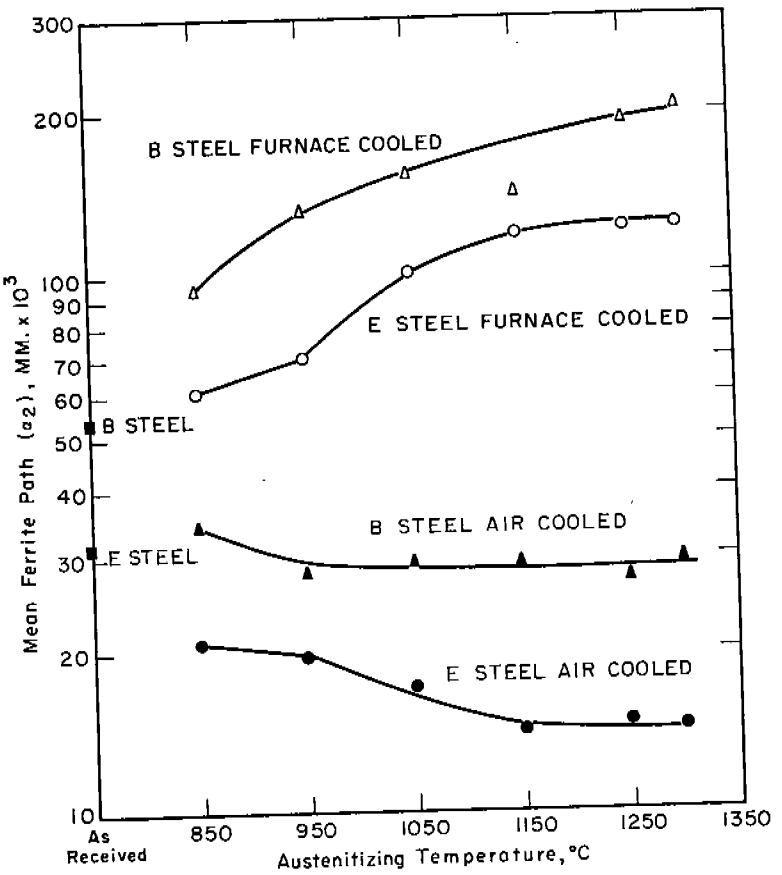

FIG. II.9 - VARIATION OF THE MEAN FERRITE PATH (α_2) WITH AUSTENITIZING TEMPERATURE FOR THE FURNACE AND AIR-COOLED SERIES

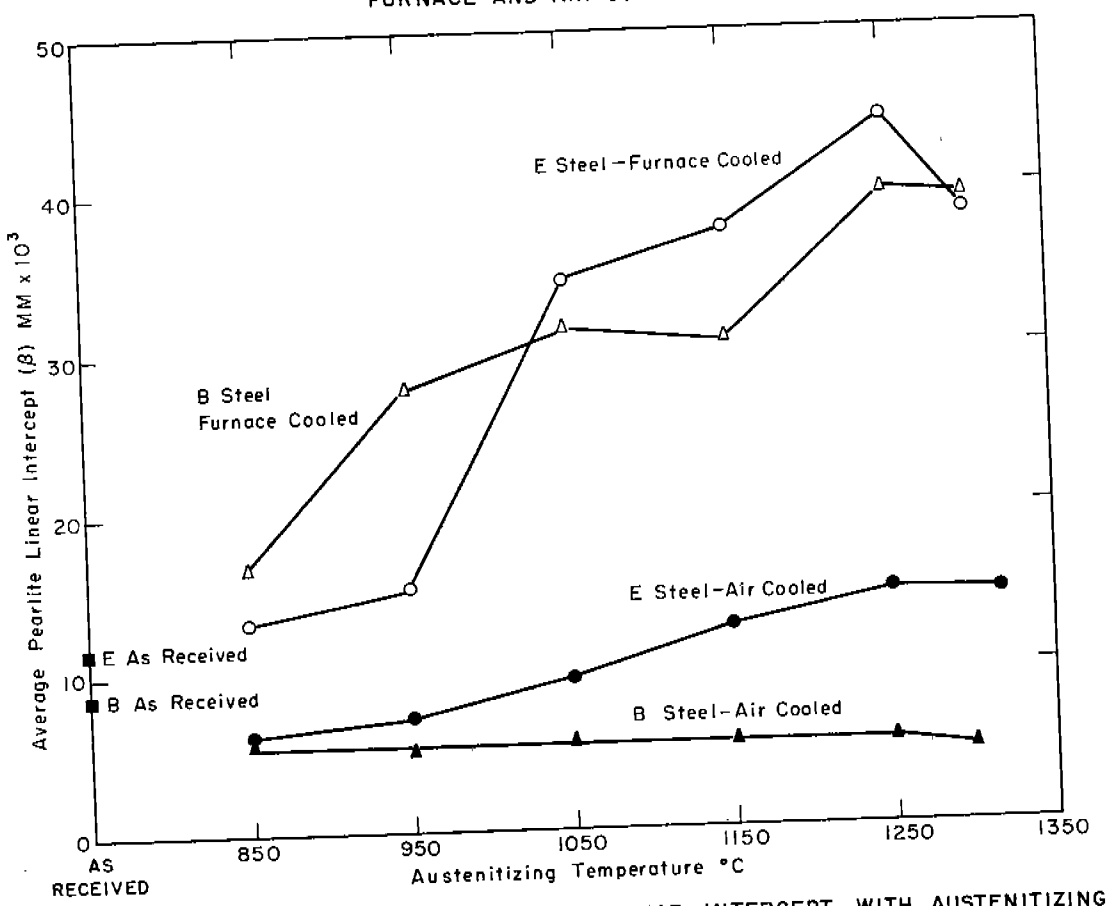

FIG. II.10 - VARIATION OF AVERAGE PEARLITE LINEAR INTERCEPT WITH AUSTENITIZING TEMPERATURE.

TABLE II-2

MEANS AND STANDARD DEVIATIONS OF MICROSTRUCTURAL PARAMETERS AND CHARPY TRANSITION TEMPERATURES

		V-NOTCH CHARPY TRANSITION TEMPERATURE (10 FT-LB LEVEL)		FERRITE GRAIN SIZE (10 GRAINS PER mm^3)						MEAN-FERRITE PATH (a_1) (mm x 10^3)						MEAN FERRITE PATH (a_2) (mm x 10^3)					
STEEL	TREAT-MENT	MEAN VALUE (T_m)	STD. DEV.	PARAL-LEL	STD. DEV.	PERPEN-DICULAR	STD. DEV.	AVER-AGE**	STD. DEV.	PARAL-LEL	STD. DEV.	PERPEN-DICULAR	STD. DEV.	AVER-AGE**	STD. DEV.	PARAL-LEL	STD. DEV.	PERPEN-DICULAR	STD. DEV.	AVER-AGE**	STD. DEV.
As Received Condition																					
B		-14.59°C	3.03°C	42.24	12.64	61.54	13.06	55.85	15.86	22.98	1.82	20.51	1.45	21.75	2.06	12.13	45.42	6.42	54.09	13.02	
E		15.68	3.75	69.11	23.28	86.77	23.73	79.14	26.79	20.66	2.32	18.87	1.72	19.76	2.23	6.04	29.02	3.52	31.37	5.48	
Furnace-Cooled Series																					
B	850°C	-8.14	1.12	16.15	5.89	26.25	4.35	20.39	7.84	29.77	3.62	25.32	1.40	27.55	3.53	125.43	48.16	63.93	9.18	94.68	46.34
	950°C	-2.96	1.93	3.36	1.77	8.22	2.72	5.08	3.29	50.26	8.82	37.29	4.11	43.77	9.45	191.76	74.31	76.88	14.08	134.32	78.48
	1050°C	2.21	1.88	2.45	1.17	5.53	1.75	3.58	2.11	55.80	8.90	42.56	4.50	49.18	9.67	214.61	78.64	92.02	15.81	153.31	83.51
	1150°C	8.10	3.83	2.21	0.74	2.78	0.95	2.48	0.89	57.76	6.49	53.51	6.10	55.64	6.65	166.34	70.91	119.58	37.17	142.96	61.25
	1250°C	17.00	1.31	1.84	0.73	1.71	0.54	1.78	0.64	61.40	8.15	62.88	6.56	62.14	7.43	203.32	48.39	185.62	45.70	194.47	47.89
	1300°C	19.50	1.73	1.42	0.46	1.37	0.59	1.40	0.54	66.96	7.29	67.71	9.74	67.33	8.61	200.20	62.13	207.32	49.52	203.76	56.30
E	850°C	24.09	1.49	54.04	19.71	63.80	13.83	58.65	18.44	19.91	2.42	18.84	1.36	19.37	2.03	64.94	22.03	58.42	12.89	61.68	18.34
	950°C	22.36	1.56	34.95	17.08	36.91	9.24	35.86	14.24	23.02	3.75	22.61	1.89	22.82	3.02	79.98	71.66	60.86	12.64	70.35	53.36
	1050°C	35.46	1.52	3.08	1.21	4.50	1.59	3.70	1.56	51.73	6.77	45.59	5.37	48.66	6.84	121.01	43.91	83.19	15.83	102.10	38.04
	1150°C	38.36	1.90	2.50	1.03	2.92	1.24	2.70	1.14	55.48	7.59	52.64	7.42	54.06	7.64	137.30	49.88	104.66	23.28	120.98	42.41
	1250°C	48.18	4.15	1.85	0.83	1.85	0.70	1.85	0.77	61.34	9.21	61.30	7.69	61.32	8.48	126.17	32.05	118.38	27.82	122.77	30.20
	1300°C	53.82	1.10	2.09	0.93	2.16	0.74	2.12	0.84	58.21	8.69	58.21	6.63	58.53	7.74	122.45	85.85	125.12	30.03	123.79	96.14
Air-Cooled Series																					
B	850°C	-30.14	3.12	231.35	75.66	229.66	72.71	230.22	73.84	13.76	1.50	13.74	1.45	13.75	1.47	35.28	6.01	33.56	5.46	34.42	5.80
	950°C	-23*		170.97		181.83		176.40		13.60		13.29		13.44		28.54		27.44		27.99	
	1050°C	-21*		182.75		177.17		179.96		13.43		13.37		13.40		28.73		29.81		29.27	
	1150°C	-15*		222.25		180.58		201.41		12.44		13.32		12.88		28.72		29.51		29.12	
	1250°C	-10*		144.79		150.93		147.86		14.35		14.26		14.30		27.51		27.10		27.31	
	1300°C	-7*		164.12		159.86		161.99		13.87		13.87		13.87		29.05		30.28		29.67	
E	850°C	-18.88	1.89	612.96	204.72	701.59	283.79	656.42	243.16	9.97	1.11	9.79	1.32	9.88	1.22	20.89	3.50	21.00	4.29	20.95	3.92
	950°C	-23.05	1.75	621.34	210.04	625.59	210.22	623.46	211.17	9.94	1.12	9.91	1.11	9.92	1.12	19.63	4.10	19.38	3.91	19.51	4.01
	1050°C	13*		294.31		280.24		287.28		11.32		11.51		11.42		16.72		17.48		17.10	
	1150°C	16*		378.41		459.92		419.16		10.41		9.77		10.09		14.57		13.59		14.08	
	1250°C	33*		410.44		356.61		383.53		10.15		10.64		10.40		13.47		15.92		14.69	
	1300°C	38*		431.22		561.09		496.16		9.96		9.13		9.55		16.34		12.53		14.44	

* ESTIMATED FROM CHARPY TRANSITION CURVE

** AVERAGE OF PARALLEL AND PERPENDICULAR

TABLE II-2 (cont'd)

MEANS AND STANDARD DEVIATIONS OF MICROSTRUCTURAL PARAMETERS AND CHARPY TRANSITION TEMPERATURES

		V-NOTCH CHARPY TRANSITION TEMPERATURE (10 FT-LB LEVEL)		PEARLITE LINEAR INTERCEPT (β) (mm x 10^3)						VOLUME FRACTION OF FERRITE						VOLUME FRACTION OF PEARLITE					
STEEL	TREAT-MENT	MEAN VALUE(T_m)	STD. DEV.	PARAL-LEL	STD. DEV.	PERPEN-DICULAR	STD. DEV.	AVER-AGE**	STD. DEV.	PARAL-LEL	STD. DEV.	PERPEN-DICULAR	STD. DEV.	AVER-AGE	STD. DEV.	PARAL-LEL	STD. DEV.	PERPEN-DICULAR	STD. DEV.	AVER-AGE**	STD. DEV.
As Received Condition																					
B		−14.59°C	3.03°C	10.08	1.41	7.69	0.80	8.89	1.65	0.8530	0.0511	0.8532	0.0216	0.8531	0.0392	0.1470	0.0511	0.1468	0.0216	0.1469	0.0392
E		15.68	3.75	10.70	1.29	9.64	1.26	10.17	1.38	0.7559	0.0355	0.7485	0.0328	0.7522	0.0344	0.2441	0.0355	0.2515	0.0328	0.2478	0.0344
Furnace-Cooled Series																					
B	850°C	−8.14	1.12	23.45	6.14	10.14	1.18	16.80	7.99	0.8323	0.0461	0.8611	0.0235	0.8467	0.0393	0.1677	0.0461	0.1389	0.0235	0.1533	0.0393
	950°C	−2.96	1.93	42.38	10.55	12.93	3.20	27.66	16.66	0.8033	0.0672	0.8543	0.0302	0.8288	0.0580	0.1967	0.0672	0.1457	0.0302	0.1712	0.0580
	1050°C	2.21	1.88	47.18	16.77	15.58	3.56	31.38	19.92	0.8322	0.0529	0.8534	0.0317	0.8428	0.0449	0.1678	0.0529	0.1466	0.0317	0.1572	0.0449
	1150°C	8.10	3.83	37.67	13.85	23.35	4.75	30.51	12.59	0.8076	0.0574	0.8264	0.0506	0.8170	0.0549	0.1924	0.0574	0.1736	0.0506	0.1830	0.0549
	1250°C	17.00	1.31	44.18	10.51	35.28	9.32	39.73	10.89	0.8163	0.0496	0.8354	0.0457	0.8258	0.0487	0.1837	0.0496	0.1646	0.0457	0.1742	0.0487
	1300°C	19.50	1.73	40.40	10.79	38.10	11.40	39.25	9.72	0.8287	0.0432	0.8408	0.0467	0.8348	0.0454	0.1713	0.0432	0.1592	0.0467	0.1652	0.0454
E	850°C	24.09	1.49	14.90	3.20	11.52	1.62	13.21	3.05	0.7996	0.0679	0.8304	0.0348	0.8150	0.0561	0.2004	0.0679	0.1696	0.0348	0.1850	0.0561
	950°C	22.36	1.56	16.87	6.09	13.20	1.98	15.12	4.96	0.7749	0.1406	0.8178	0.0335	0.7953	0.1066	0.2251	0.1406	0.1822	0.0335	0.2047	0.1066
	1050°C	35.46	1.52	41.61	11.14	27.25	4.77	34.43	11.18	0.7308	0.0801	0.7505	0.0439	0.7407	0.0653	0.2692	0.0801	0.2495	0.0439	0.2593	0.0653
	1150°C	38.36	1.90	40.64	10.79	34.48	7.33	37.56	9.72	0.7567	0.0775	0.7488	0.0503	0.7528	0.0655	0.2433	0.0775	0.2512	0.0503	0.2472	0.0655
	1250°C	48.18	4.15	46.52	9.44	42.37	10.07	44.44	9.98	0.7257	0.0535	0.7338	0.0637	0.7298	0.0589	0.2743	0.0535	0.2662	0.0637	0.2702	0.0589
	1300°C	53.82	1.10	40.89	12.61	35.70	8.71	38.29	9.32	0.7468	0.0436	0.7112	0.0596	0.7590	0.0536	0.2532	0.0436	0.2288	0.0596	0.2410	0.0536
Air-Cooled Series																					
B	850°C	−30.14	3.12	5.78	0.54	5.60	0.62	5.69	0.59	0.8569	0.0207	0.8549	0.0210	0.8559	0.0209	0.1431	0.0207	0.1451	0.0210	0.1441	0.0209
	950°C	−23*		5.25		4.92		5.09		0.8446		0.8480		0.8463		0.1554		0.1520		0.1537	
	1050°C	−21*		5.69		5.56		5.63		0.8319		0.8416		0.8368		0.1681		0.1584		0.1632	
	1150°C	−15*		5.15		5.54		5.35		0.8469		0.8408		0.8439		0.1531		0.1592		0.1561	
	1250°C	−10*		5.24		5.51		5.38		0.8398		0.8308		0.8353		0.1602		0.1692		0.1647	
	1300°C	−7*		4.76		4.83		4.80		0.8591		0.8611		0.8601		0.1409		0.1389		0.1399	
E	850°C	−18.88	1.89	6.31	0.59	6.08	0.55	6.20	0.58	0.7644	0.0359	0.7702	0.0381	0.7673	0.0372	0.2356	0.0359	0.2298	0.0381	0.2327	0.0372
	950°C	−23.05	1.75	7.25	0.82	7.26	0.71	7.26	0.76	0.7233	0.0594	0.7209	0.0573	0.7221	0.0584	0.2767	0.0594	0.2791	0.0573	0.2779	0.0584
	1050°C	13*		9.35		9.98		9.67		0.6413		0.6387		0.6400		0.3587		0.3613		0.3600	
	1150°C	16*		12.81		12.73		12.77		0.5339		0.5156		0.5248		0.4661		0.4844		0.4752	
	1250°C	33*		13.47		15.92		14.69		0.4978		0.4810		0.4894		0.5022		0.5190		0.5106	
	1300°C	38*		16.34		12.53		14.44		0.4201		0.4967		0.4584		0.5799		0.5033		0.5416	

*ESTIMATED FROM CHARPY TRANSITION CURVE

**AVERAGE OF PARALLEL AND PERPENDICULAR

almost identical ferrite grain size was produced in the two steels by the same annealing treatment.

The results for the E steel specimens annealed at 850° C do not follow the smooth curves through the data from the other specimens in the series. It may be that the temperature was too low to insure complete austenitization in one hour.

In the air-cooled series, Widmanstatten structures were found in the B specimens austenitized at 950° C and above, and in the E specimens at 1050° C and above. Due to the change in ferrite morphology, comparisons of the n_v, α_1, α_2 and β parameters of equiaxed structures with those of the Widmanstatten structures are not quantitatively exact. However, in a general way the data plotted in Figs. II.7 to II.10 demonstrate that air cooling refined the structure. Normalizing at any temperature in the range 850°--1300° C produced a finer structure in the E steel than in the B. All the parameters were remarkably insensitive to the normalizing temperature.

The measured volume fraction of pearlite (listed in Table II.2) indicated a difference in the transformational behavior of the two steels. The volume percentage of pearlite in the B steel was constant, within the limits of statistical variability, for furnace and air cooling. In contrast, the amount of pearlite in the E steel was increased by as much as a factor of two by altering the cooling rate from furnace to air cooling. The behavior of the E steel is in line with the general observation[58] that the amount of pearlite increases with increasing cooling rate. Thus, the B steel

appears to be unusual. At least a partial explanation may be that the higher manganese content of the B steel renders it relatively insensitive to cooling rate. This contention is supported by the observation that raising the manganese content decreases the slopes of the proeutectoid ferrite and pearlite C -curves in the isothermal transformation diagrams[59].

The pearlite patch size β (Fig. II.10) exhibited practically the same increase with austenitizing temperature in both annealed steels, but a divergence appeared in the normalized series. In the latter, the β parameter increased in the E steel (as did the amount of pearlite) but was insensitive to the normalizing temperature in the B steel.

Furnace cooling from an austenitizing temperature in the range 850°--1150° C resulted in a banded structure which was more prevalent in the B steel. This appears to be a further manifestation of the higher manganese content of this steel. The extent of banding in the two steels is shown in Fig. II.11, in which the ratio of the average pearlite intercept (β) measured parallel and perpendicular to the rolling surface (on a transverse section) and the corresponding ratio of mean ferrite path (α_2) are plotted against austenitizing temperature.

<u>Variation of Charpy transition temperature with heat treatment.</u> The 10 ft-lb V-notch Charpy transition temperatures are plotted as a function of the austenitizing temperature in Fig. II.12. The B steel data generally lay about 34° C below that for the E steel.

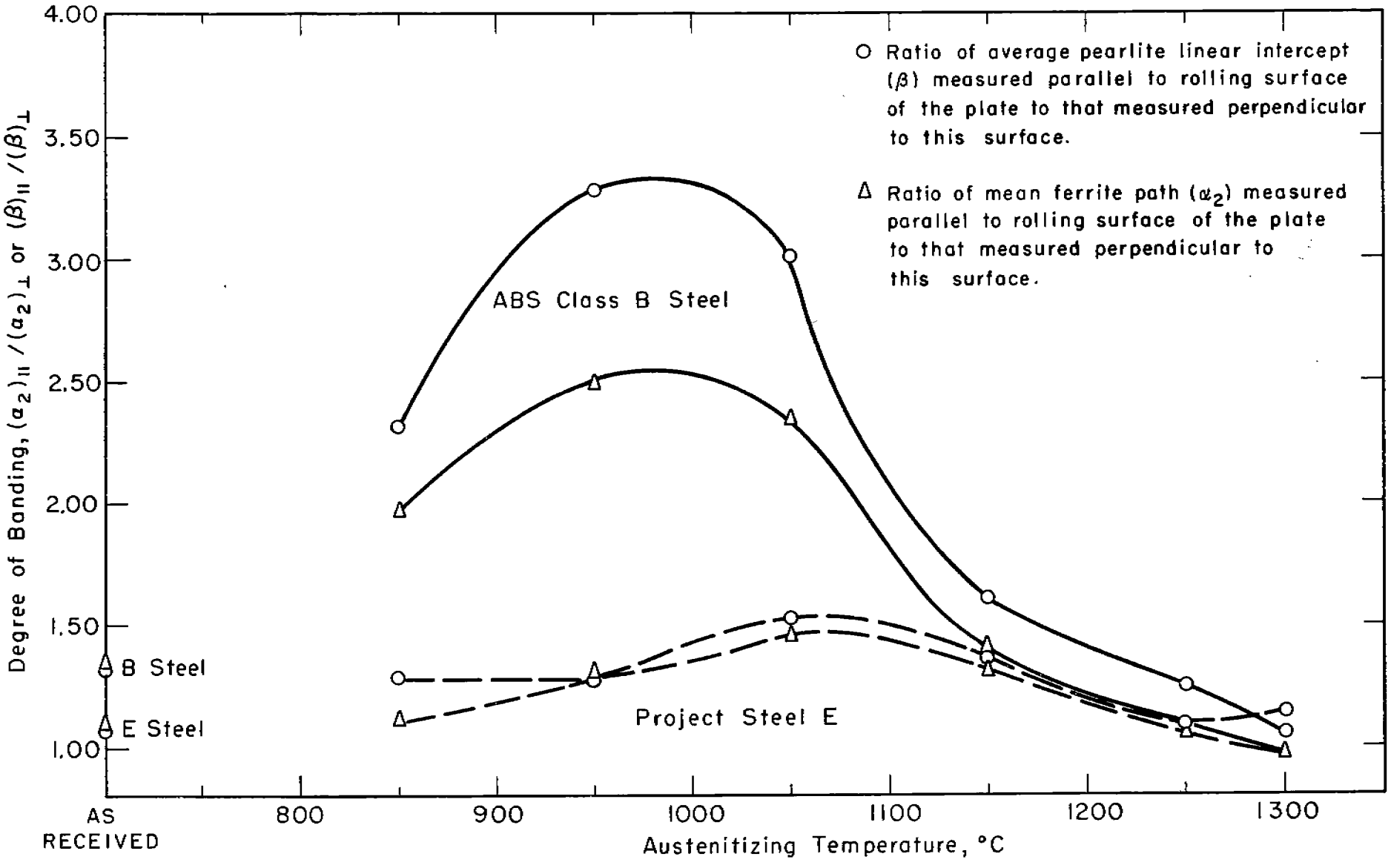

FIG. II.11 - RELATIONSHIP BETWEEN THE DEGREE OF BANDING ON TRANSVERSE SECTIONS AND THE AUSTENITIZING TEMPERATURE FOR THE FURNACE-COOLED SERIES.

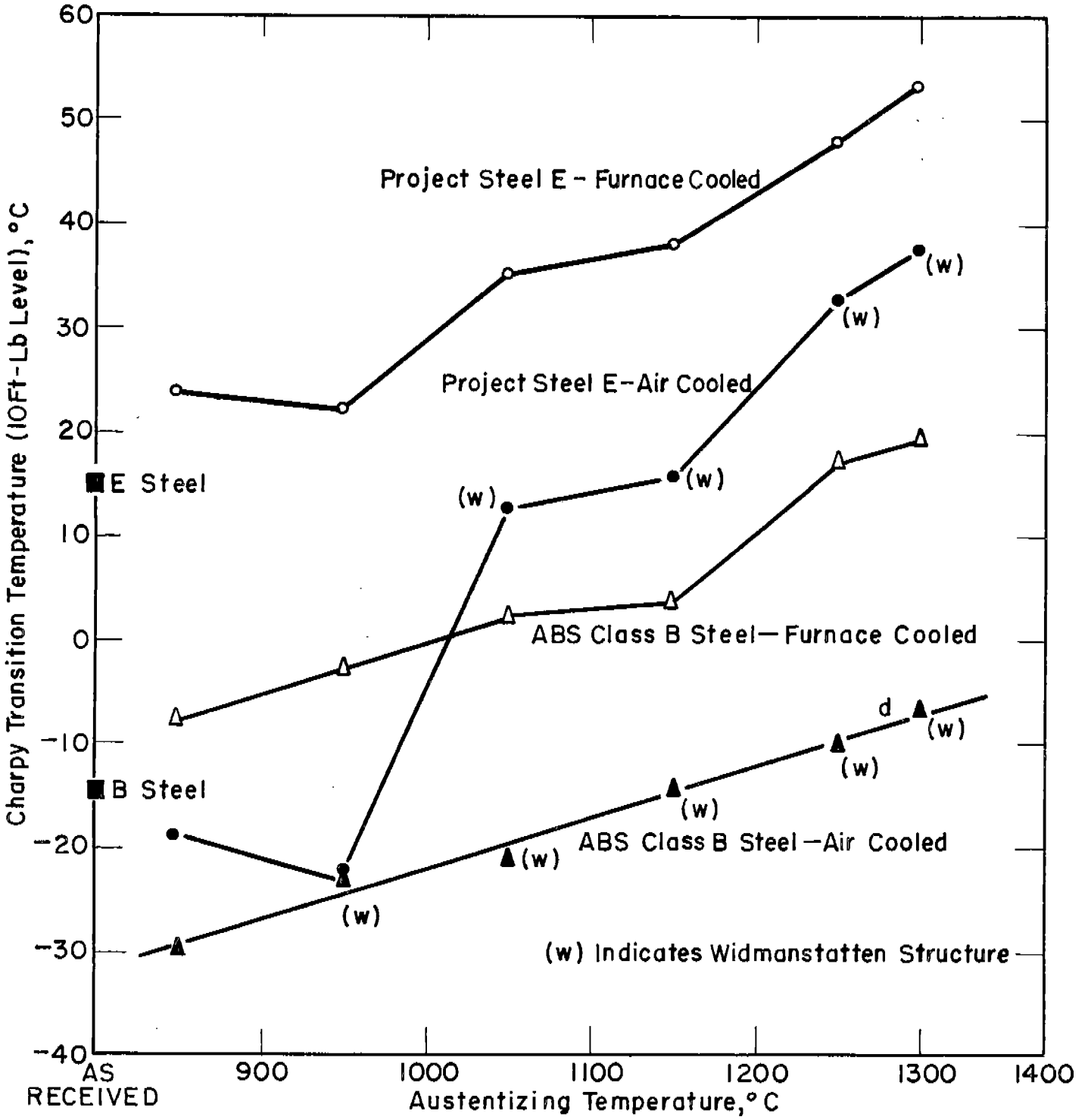

FIG. II 12 - EFFECT OF AUSTENITIZING TEMPERATURE ON THE CHARPY TRANSITION TEMPERATURE FOR THE FURNACE AND AIR-COOLED SERIES

The transition temperatures of both steels were lowered by air cooling compared to furnace cooling and increased with the austenitizing temperature.

The behavior of the E steel was remarkable, in that after air cooling from 850°--950° C, which gave equiaxed ferrite, the transition temperatures were only slightly higher than for the corresponding B steel specimens. From higher austenitizing temperatures the transition temperature of the E steel rose sharply, accompanied by Widmanstatten structures and a marked increase in the amount of pearlite.

Correlation of microstructure with Charpy transition behavior.

In the case of the furnace-cooled series, statistical methods were applied to the problem of relating microstructure to Charpy transition behavior. The microstructural parameters used were those measured perpendicular to the plate surface, that is, in the same direction as the V-notch of the Charpy bar. This selection was suggested by the results of Harris and co-workers[60] who, by using low energy repeated blow tests, showed that the crack initiated near the root of the notch and spread laterally before propagating catastrophically across the specimen. It was found that this method of treating the data gave better correlations than when the microstructural parameters were averaged between the perpendicular and parallel directions to the plate surface; however, the overall trends were not materially affected.

The application of statistical methods was greatly simplified by assuming linear relationships between the microstructural parameters and the 10 ft-lb Charpy transition temperature. The experimental data (Figs. II.13 to II.16) showed that this assumption was justified. Regression analysis was used[54]; that is, the frequency distribution of the Charpy transition temperature was considered when the independent variable, one of the microstructural parameters, was held fixed at its mean value. The results of regression analysis are shown in Figs. II.13 to II.16. Included are the 95% confidence intervals for the empirical regression line and the 95% confidence limits for the mean values of the transition temperature and microstructural parameters.

The empirical regression lines for the ferrite grain size plot (Fig. II.13) indicate that in the case of the E steel an increase of one ASTM grain size number corresponded to a decrease in transition temperature of 8° C (14.4° F). The figure for the B steel was 10° C (18° F). A decrease of 11° C (20° F) in keyhole Charpy transition temperature per grain size number has been reported by Battelle investigators[39] and Vanderbeck[40] for annealed semikilled steels.

The Charpy transition temperature of both steels was raised by increasing the mean ferrite path, α_1 or α_2, and the pearlite linear intercept β. A comparison of the individual slopes of the regression lines in Figs. II.13 to II.16 revealed these microstructural parameters had essentially the same influence

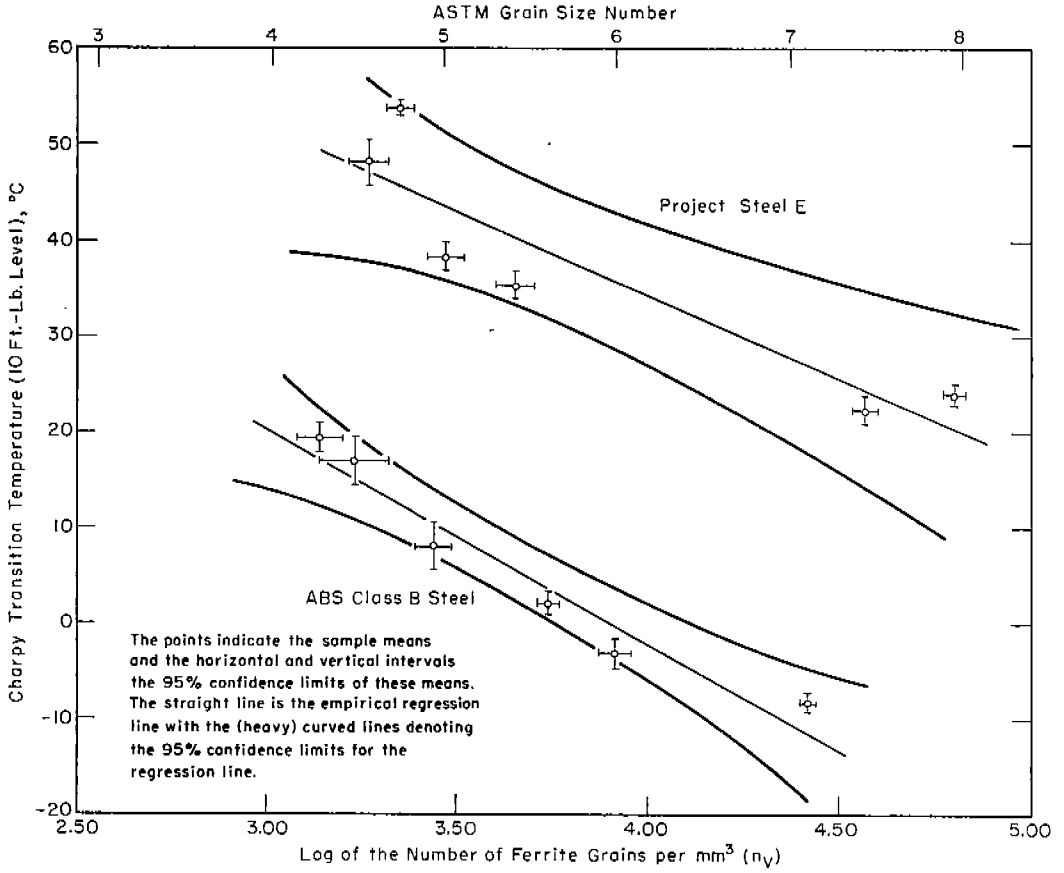

FIG.II.13-RELATIONSHIP BETWEEN FERRITE GRAIN SIZE AND CHARPY TRANSITION TEMPERATURE FOR THE FURNACE-COOLED SERIES.

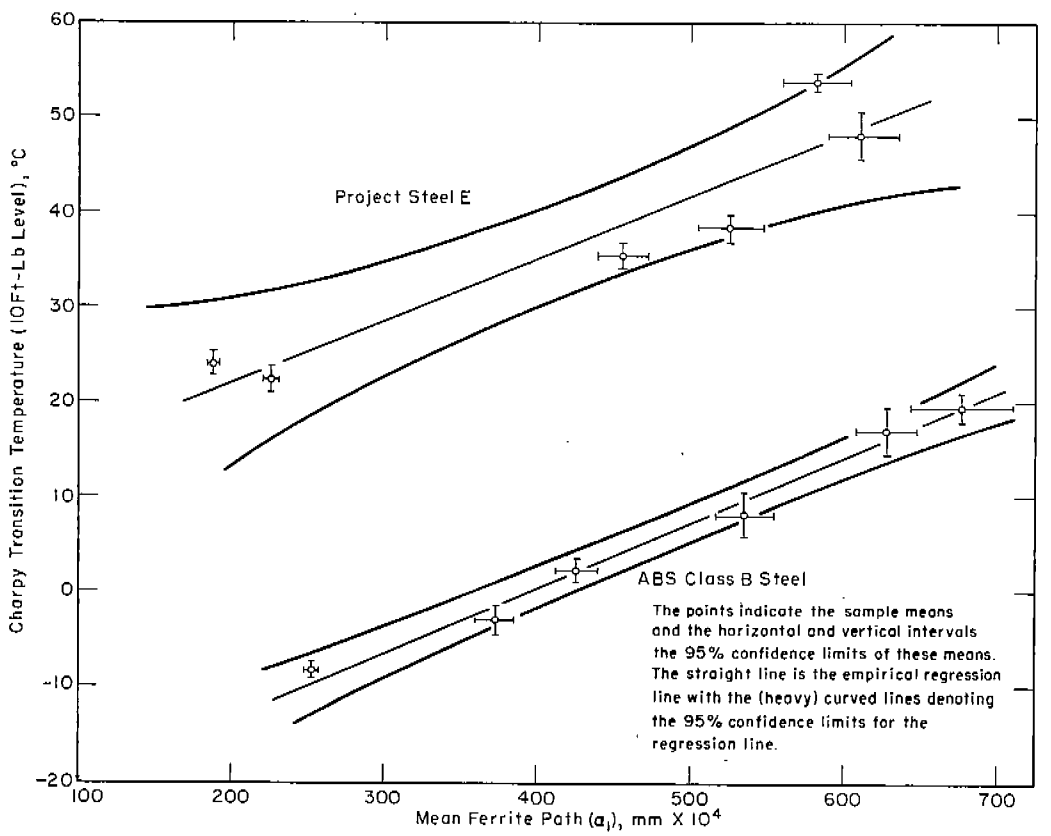

FIG.II.14- RELATIONSHIP BETWEEN THE MEAN FERRITE PATH, α_1, AND THE CHARPY TRANSITION TEMPERATURE FOR THE FURNACE-COOLED SERIES.

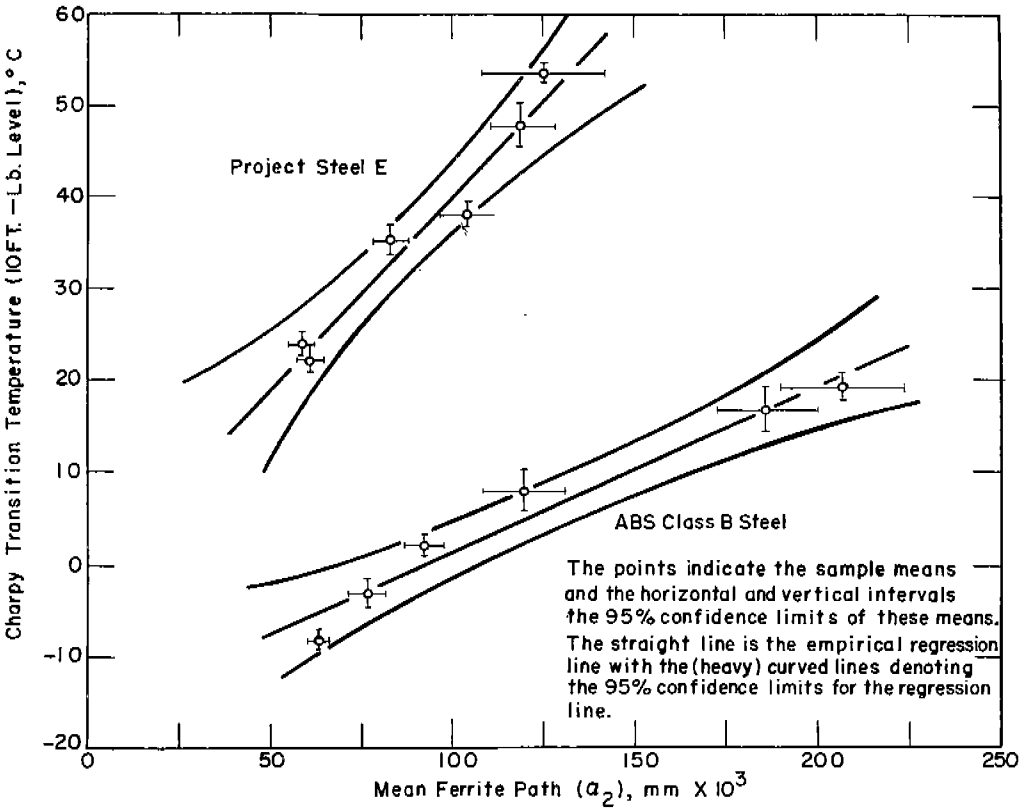

FIG. II 15 - RELATIONSHIP BETWEEN THE MEAN FERRITE PATH, a_2, AND THE CHARPY TRANSITION TEMPERATURE FOR THE FURNACE-COOLED SERIES.

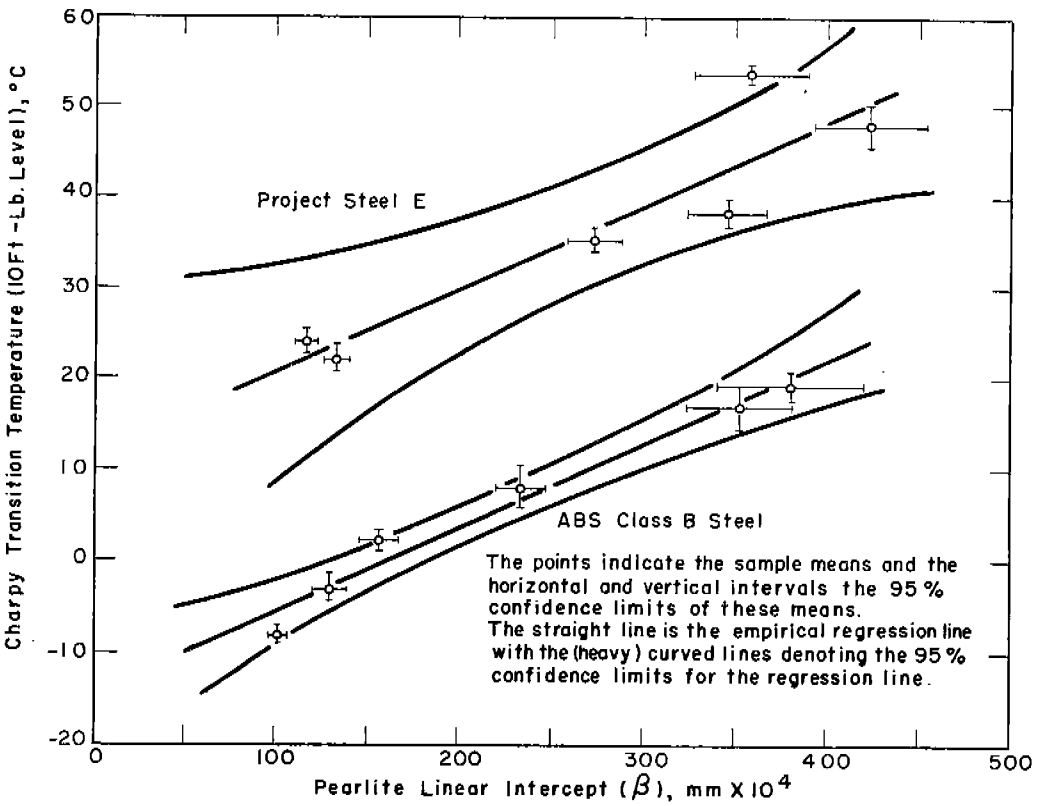

FIG. II. 16 - RELATIONSHIP BETWEEN THE PEARLITE INTERCEPT, β, AND THE CHARPY TRANSITION TEMPERATURE FOR THE FURNACE-COOLED SERIES.

on the transition temperatures of the two steels, except for the mean ferrite path, α_2. In this case the slope for the E steel is more than twice that for the B steel, but the reason is unclear.

The ferrite parameters n_v and α_1 are expicitly related (Eqs. 1 and 4). In the furnace-cooled series both these parameters and the pearlite intercept are simple functions of the austenitizing temperature. Consequently, all three parameters, n_v, α_1 and β, are interdependent. Thus, to assess the strength of the correlations between these microstructural variables and the transition temperature, it was necessary to consider the "partial" correlation coefficients. For two variables (the transition temperature and one microstructural parameter), these coefficients are obtained by fixing all other related variables. Such a study[54] showed that, for the two steels examined, the ferrite parameters, n_v or α_1, (i.e., the ferrite grain size), were better parameters for estimating the V-notch Charpy transition temperature than the pearlite patch size.

The presence of pearlite banding proved not to be a major factor in influencing the transition temperature. As shown in Fig. II.17, both high and low transition temperatures corresponded to a given degree of banding. From this it can be inferred that the banding, as well as the α_2 and β parameters used to measure it, were of secondary importance here, being masked by other more powerful effects. Undoubtedly, the functional relationship between the transition temperature and ferrite path α_2 (Fig. II.15) or pearlite

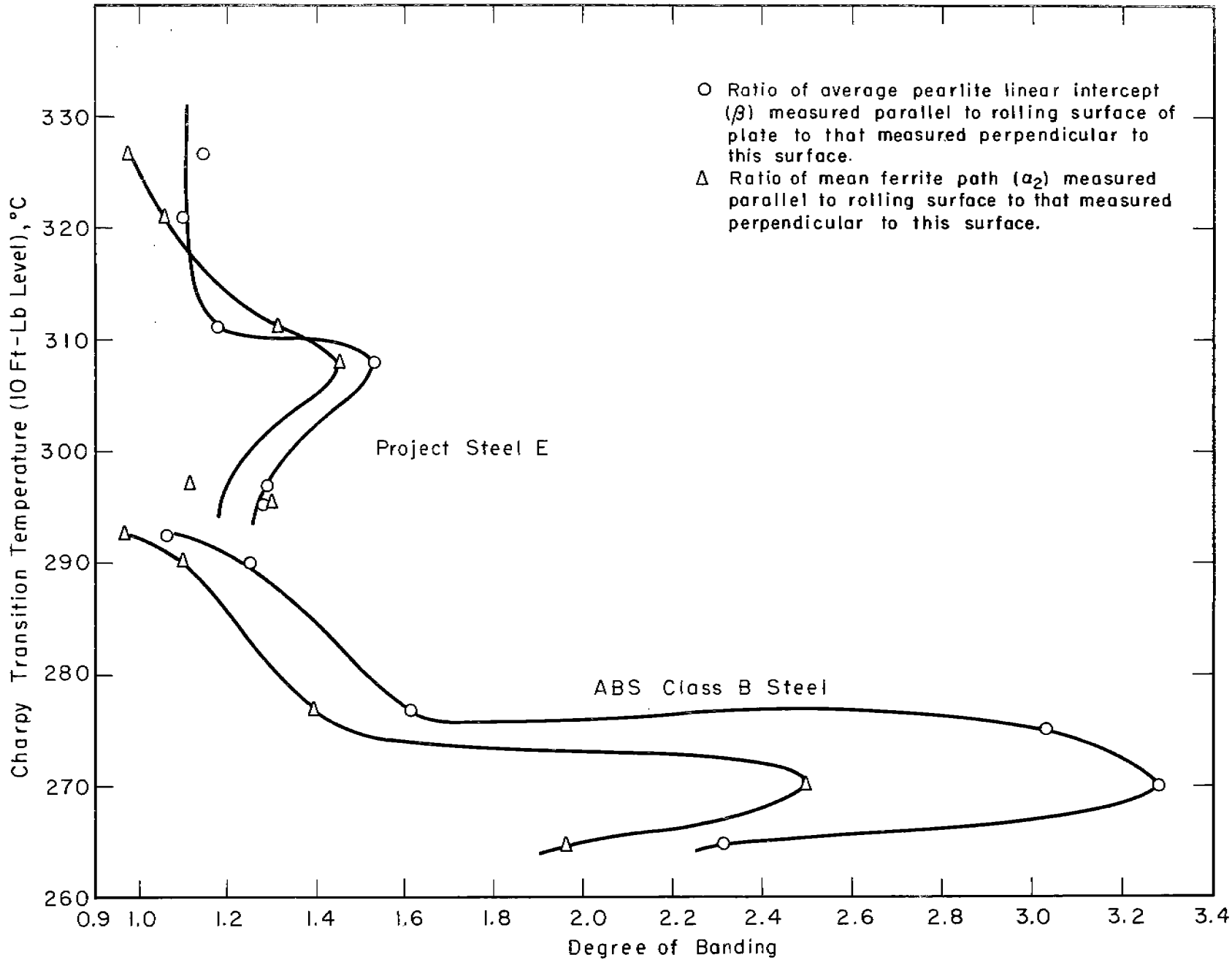

FIG. II.17 – RELATIONSHIP OF CHARPY TRANSITION TEMPERATURE TO THE DEGREE OF BANDING FOR THE FURNACE-COOLED SERIES.

patch size β (Fig. II.16) resulted from the unavoidable circumstance that the ferrite grain size (and perhaps other factors) underwent simultaneous changes as the α_2 and β parameters were being varied by heat treatment.

Another secondary factor was the amount of pearlite. However, as pointed out in the following discussion, it was possible to sort out the influence of this variable on the transition temperature, at least in an approximate way. Except for the air-cooled E specimens, the percentage of pearlite was insensitive to the heat treatments employed.

Inasmuch as the mean ferrite path α_1 (or ferrite grain size) appeared to be the most powerful parameter in determining the transition temperature, it provided a useful basis for comparing the transition behavior of air- and furnace-cooled specimens. The results are collected in Fig. II.18. The furnace-cooled series are represented by the regression lines previously introduced. The low-temperature air-cooled specimen data are the mean transition temperatures (T_m) shown in Table II.2. For specimens with Widmanstatten structures, the values were taken directly from the Charpy transition curves.

DISCUSSION OF RESULTS

For each steel furnace cooled from a range of austenitizing temperatures, the Charpy V-notch transition temperature varied systematically with changes in microstructure. The dominant

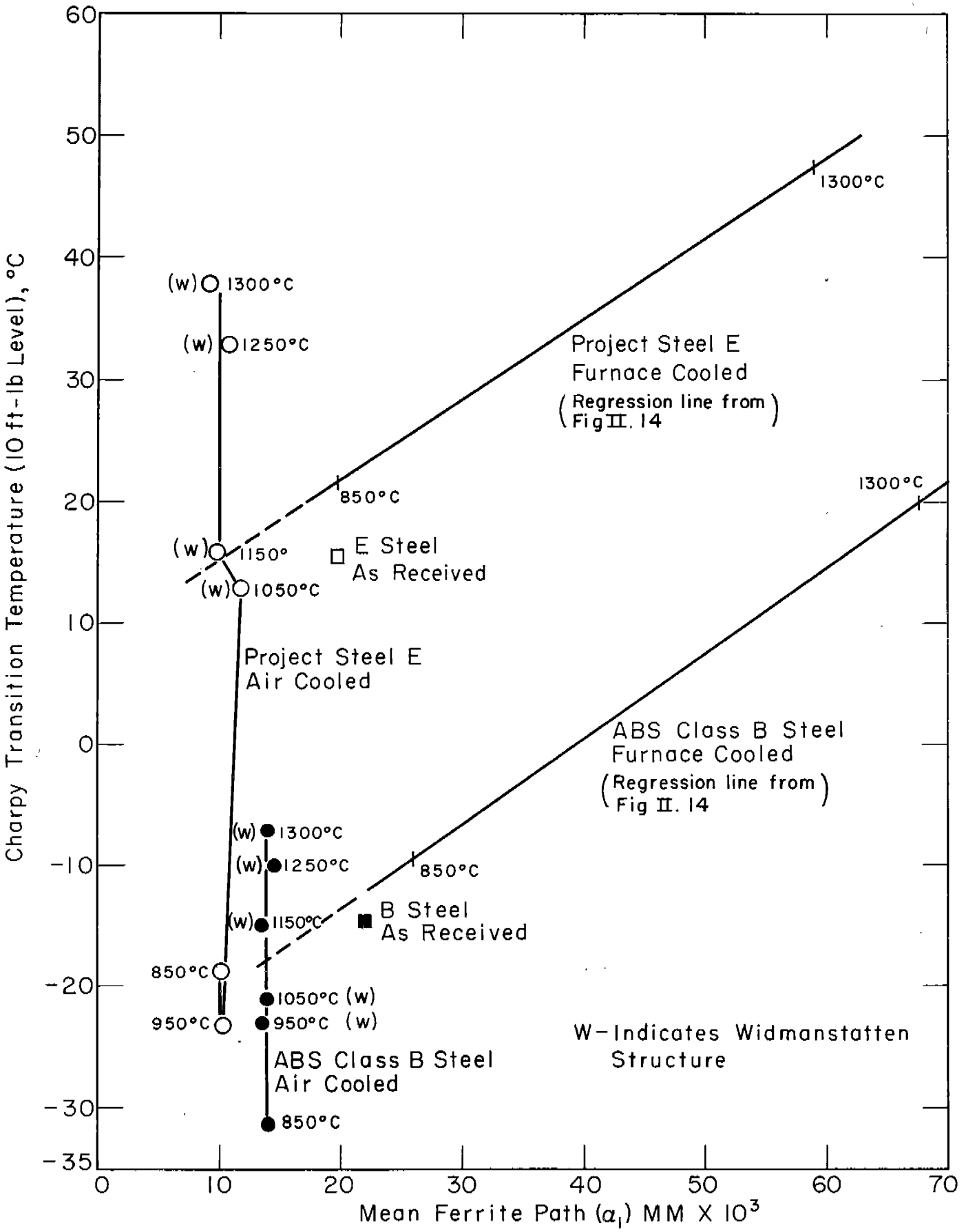

FIG. II.18 - RELATIONSHIP BETWEEN THE MEAN FERRITE PATH, α_1, AND CHARPY TRANSITION TEMPERATURE

microstructural feature was the parameter α_1 (or the ferrite grain size). The correlation between the transition temperature and this parameter was linear to a remarkable degree of confidence.

All the data relating the α_1 parameter to transition temperature are assembled in Fig. II.18. By a short extrapolation, air-cooled and furnace-cooled steels of the same α_1 parameter can be compared. A small correction is required because of differences in the amount of pearlite. It is possible to estimate the effect of a change in the percentage of pearlite on the transition temperature by considering the data for the air-cooled series between 1050° C and 1300° C (Table II.2). Over this range the structure was Widmanstatten, and the α_1, α_2, n_v and β parameters did not change appreciably with austenitizing temperature. For the B steel the amount of pearlite was constant at about 15%, but the transition temperature increased 14° C. However, for the E steel the pearlite increased by 18% (from 36 to 54%) while the transition temperature increased 25° C over the same range of austenitizing temperatures. If it is assumed that, when the percentage of pearlite in the two steels remains constant, the effect of raising the austenitizing temperature as such is the same for both steels*,

*This assumption seems reasonable because the change in transition temperature with austenitizing temperature was the same for both steels in the furnace-cooled state, where the amount of pearlite was relatively insensitive to the austenitizing temperature.

the further increment in transition temperature for the E steel can be attributed to the increase in pearlite. On this basis, an increase of 11° C in transition temperature is produced by an increase of 18% in the amount of pearlite, that is, about 0.6° C per 1%.

For the furnace-cooled series, the difference in transition temperature of the two steels was about 34° C. The average percentage of pearlite was greater by about 7% in the E steel. Since reducing the amount of pearlite lowers the transition temperature, the 34° C difference is an overestimate. However, as discussed above, correction for the additional pearlite in the E steel will probably reduce this figure by only 4° C.

According to Fig. II.18, air-cooled specimens with a predominantly equiaxed ferrite structure (austenitized below 950° C) had a lower transition temperature than a hypothetical furnace-cooled specimen of the same steel with the same α_1 value. The differences are listed in Table II.3. The extent of the improvement was considerably greater in the E steel. The change in cooling rate produced little variation in the amount of pearlite in the B steel, but in the E steel air cooling increased the pearlite by as much as 9.8% compared to furnace cooling. However, since this acts in the direction of increasing the transition temperature, it is evident that, if it were possible to compare specimens with the same α_1 and percentage pearlite, the improvement in transition

TABLE II.3

COMPARISON OF THE TRANSITION TEMPERATURE IN AIR- AND FURNACE-COOLED SPECIMENS

Steel	Austenitizing Temperature °C	Difference between 10 ft-lb Transition Temperature of Air- and Furnace-Cooled Specimens with the same Value of α_1 °C	Volume Percentage of Pearlite Furnace-Cooled (Estimated)	Air Cooled
B	850	10.3	15	14.4
	950	5.0	15	15.4
E	850	30.4	18	23.3
	950	30.9	18	27.8

temperature for the E steel would be even greater than shown in Table II.3.

On air cooling from temperatures above 950° C, the transition temperature increased with increasing austenitizing temperature and was raised into a range comparable with that of the annealed specimens. This effect coincided with the appearance of Widmanstatten structures, and in the E steel, with a marked increase in the percentage of pearlite. The microstructural parameters of the Widmanstatten structures in both steels showed very little dependence on austenitizing temperature. Nevertheless, the Charpy transition temperature increased with increasing austenitizing temperature (Fig. II.18). This suggests that the effects of austenitizing temperature, like those of chemistry (nature of the steel) and cooling

rate, are at least partly submicroscopic. For the E steel the foregoing argument is not so clear because the amount of pearlite on air cooling changed with the austenitizing temperature. However, even here it seems improbable the pearlite variations could account completely for the increase in transition temperature with the austenitizing temperature.

To account for the changes produced by altering the composition or the cooling rate, structural characteristics other than those assessed in this investigation must be examined. One of the remaining features which can be observed under the optical microscope is the interlamellar spacing of the pearlite. However, there is good reason to believe that within the range of structures being considered, this effect is negligible[42--44]. Thus, it is necessary to determine the effect on the transition temperature of such factors as carbides of ultrafine dispersion, grain boundary condition, ferrite substructure and spacial distribution of carbon and manganese atoms. These submicroscopic phenomena will be the subject of future investigations.

CONCLUSIONS

1. Correlations between microstructure and V-notch Charpy transition temperature exist only when the composition and cooling rate are defined. A change in either of these affects the transition temperature to a much greater extent than would be anticipated from a consideration of the microscopic variables alone. Thus, there

must be other powerful structural variables acting which to date have not been identified. Moreover, these submicroscopic phenomena appear to be affected by austenitizing temperature.

2. In annealed structures the transition temperature increases with the mean ferrite path and pearlite patch size. The V-notch Charpy transition temperature increases linearly with the ferrite grain size as expressed in ASTM numbers.
3. The ferrite-dependent microstructural parameters in annealed structures correlate better with the Charpy transition temperature than those which are pearlite-dependent as judged by statistical tests of significance.
4. The ferrite grain size, pearlite patch size, and austenite grain size in annealed structures are interrelated, the ferrite grain size and pearlite patch size increasing with the austenite grain size.
5. Banding, as varied by annealing treatments, is not a dominant microstructural factor in influencing the transition temperature of the ship steels studied.
6. Air cooling from above about 950° C results in Widmanstatten ferrite structures but with the following exception--the microstructural parameters are relatively insensitive to variation in the austenitizing temperature. In the more brittle steel the volume fraction of pearlite increases markedly with increasing austenitizing temperature, and there is an associated increase in the transition temperature. The appearance of a Widmanstatten structure also coincides with an increase in the transition temperature.

PART III

THE TENSILE PROPERTIES AT -195° C

INTRODUCTION

Although low temperature uniaxial tension experiments have not received the attention that has been devoted to the Charpy test, a number of investigators have recognized that it is potentially capable of providing more fundamental information concerning metallurgical aspects of brittle fracture. The general background and earlier references are given by Klier and Gensamer[63]. Several aspects of the test have been examined over limited ranges of temperature, composition and grain size; but the picture is far from complete.

The existence in iron and mild steel of a tensile ductile-brittle transition at a temperature in the general vicinity of liquid nitrogen temperature has been demonstrated[64--66]. However, no detailed investigation of this as a function of metallurgical variables in mild steel has been reported. Gensamer[63,64], Brick[2], and others have measured the strain-hardening exponent in ship steel and high purity low-carbon alloys as a function of temperature and attempted to relate it to the fracture behavior . However, the connection appears to be elusive.

All the investigations considering heat-treatment variables have been confined to one testing temperature, usually -195° C. The only microscopic parameter examined in detail has been ferrite grain size. Experimental data relating grain size to fracture and yield stress at liquid nitrogen temperature have been published by Low[23] for a very low carbon steel and by Petch[61--67] who used

specimens within the range 0.036--0.155% C, 0.005--0.59% Mn. Both changed the grain size by supercritical heat treatments and found that straight line plots were obtained when the fracture stress was plotted against the reciprocal square root of the average grain diameter ($d^{-\frac{1}{2}}$). A straight line of different slope was obtained when the yield stress was plotted against the same function. (Hall[68] had previously shown a $d^{-\frac{1}{2}}$ dependence for the lower yield point of iron tested at room temperature.)

An important difference may be noted in the interpretation of the data in the above two investigations. Low considered that his results were best represented by two lines which intersected at a value of about $d^{-\frac{1}{2}} = 2.5\ mm^{-\frac{1}{2}}$. This might be taken to be a brittle-ductile grain size transition point at a given temperature. When the reduction of area at fracture was plotted against the same function, a corresponding transition curve was obtained. On the other hand, no discontinuous transition in the fracture stress as a function of grain size was implied by Petch. By making a somewhat arbitrary correction to the fracture stress to allow for deformation prior to fracture, and giving greater weight to the large grain size results which had the smaller correction, his fracture stress and yield point curves were shown as intersecting at $d^{-\frac{1}{2}} = o$, i.e., at the yield stress of a single crystal. However, the plots of reduction in area at fracture against $d^{-\frac{1}{2}}$ showed a transition similar to that reported by Low.

Brick[2] et al. have demonstrated that at liquid air temperature the yield point of a high purity iron-carbon alloy containing 0.02% carbon is greatly affected by the heat treatment employed to

develop a given grain size. Elevation of the yield point was produced by increasing the austenitizing temperature and the cooling rate, these being treatments which enhanced the extent of ferrite veining. When subcritical treatments were used, a regular grain-size yield stress relationship was observed. This result appears to be in conflict with that reported by Allen[69] for high purity alloys prepared at National Physical Laboratory where it was found that the grain-size dependence of the low-temperature properties was not affected by the heat treatment used to establish the grain size.

Rees[70] has produced convincing evidence to show that, when steels with a range of carbon and manganese contents and heat treatments are considered, ferrite grain size is not the overwhelming factor determining fracture stress at -195° C. Petch[71] has agreed that composition and precipitation phenomena play a role through their effect on the yield point.

Although most attention has been paid to factors which determine the low temperature yield and fracture stress, it is probable that these quantities define the tendency to embrittlement in only a very general sense. For example, within one class of steel, such as ship steel, there is no evidence to suggest that these stresses at -195° C are the predominant factors defining the tendency toward low-temperature embrittlement. It has been implied that the important parameter is the total plastic strain (ductility) before fracture[69]. Systematic measurements of low-temperature ductility of brittle specimens appear to have been made only in work concerned with the effects

of added elements in high purity iron. Smith, Spangler, and Brick[2] found ferrite grain size to be the main factor determining the ductility of a 0.02% carbon iron at liquid air temperature, but the situation was altered greatly by the presence of carbides or pearlite in higher carbon alloys.

It appears that only isolated observations have been made of the connection between microstructure and fracture stress, yield stress, and ductility in mild steel at a temperature which insured brittle fracture. The purpose of this part of the investigation was to examine these questions. The experiments were performed at -195° C where the fractures were predominantly cleavage. However, although in the majority of specimens the ductility was very small, it should be noted that in a few instances the cleavage was preceded by appreciable plastic strain (more than 0.19). Thus there were cases in which, although from a crystallographic viewpoint the specimens could be described as brittle, on the basis of energy absorption they were not steels with a pronounced tendency toward low-energy catastrophic failure.

For ship steel it has been shown that the Charpy V-notch transition temperature is a good measure of the tendency to brittle behavior under service conditions[72]. Hence, the same steels with the same heat treatments were used for the tensile work as for the Charpy experiments reported in Part II. A comparison of the data permits an assessment of the relative importance of fracture stress, yield stress, and ductility in the tensile brittle range.

Experimental procedure. Tensile blanks were cut from the B and E steel plates with the major axis parallel to the rolling direction. Series of specimens were prepared with the same heat treatments as in the Charpy work.

The tests were carried out on a 60,000 lb. capacity hydraulic machine, axiality being insured by loading through long high-carbon steel chains[2]. The load was applied continuously with a cross-head speed of about 0.005 in. per minute. The strain over a two-in. gage length (on a 0.252 in. diameter specimen) was measured and automatically recorded by an instrument capable of detecting a change of 0.0001 in. The reduction in area of each specimen was calculated from measurements of the diameter of the specimen before and after testing. In order to attach securely the arms of the differential transformer gage, it was necessary to make two small indentations in the specimen surface. In a few instances when the specimens were extremely brittle, fracture occurred close to these marks. These results were rejected, and duplicate specimens with polished surfaces and no gage marks were tested to obtain reliable reduction-in-area data. Liquid nitrogen was used as the refrigerant.

A microspecimen was cut from each tensile blank, and the microstructural parameters were measured by the method described in Part II.

RESULTS

The only microstructural parameter for which there appeared to be any correlation with tensile properties was the mean ferrite grain size (n_v or α_1). To permit comparison with earlier work, this

was converted to the average diameter d (Eq. 4a).

All tests were carried out in triplicate. When the results showed appreciable scatter, further tests were run. All points plotted are averages.

For all specimens the upper yield point was clearly defined. Most specimens broke at, or close to, the lower yield stress. No correlations could be found with any microstructural parameter applicable to those specimens containing appreciable amounts of Widmanstatten ferrite (specimens air cooled from above 950° C). Consequently, these were excluded from the plots of yield stress and fracture stress against $d^{-\frac{1}{2}}$ (Fig. III.1 A and B). The majority of E steel specimens broke before the lower yield stress was clearly attained, and therefore only the upper yield stress points are included in Fig. III.1 B.

No microstructural parameters were found to correlate with the ductility. In Fig. III.2 the total plastic extension to fracture is shown as a function of the austenitizing temperature. The reduction of area is plotted in the same manner in Fig. III.3.

All the specimens broke with a "crystalline" cleavage fracture, with the exception of a few E steel specimens air cooled from 875° C or 950° C that necked before fracture. Five other specimens heat treated and tested in exactly the same way displayed marked ductility but did not neck. The scatter of the results was larger, the greater the average ductility.

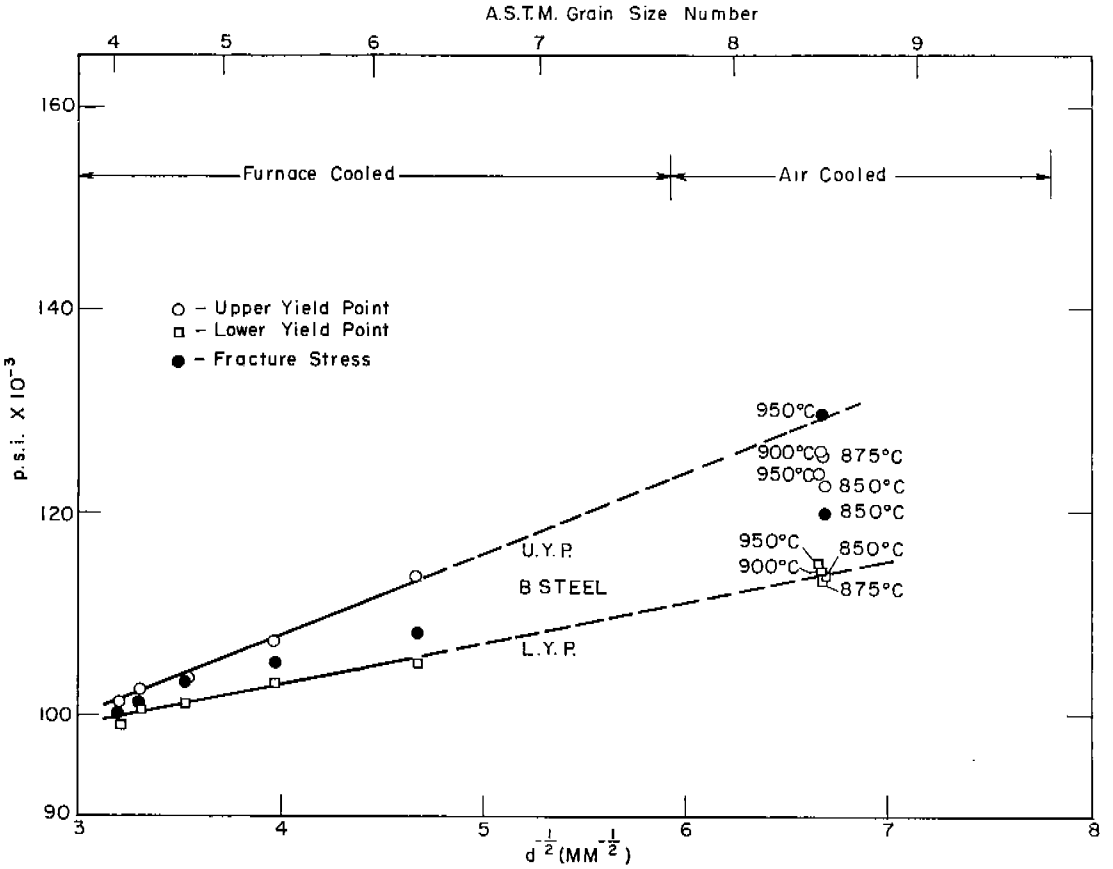

FIG. III IA-YIELD STRESS AND FRACTURE STRESS AT -195°C AS A FUNCTION OF AVERAGE FERRITE GRAIN DIAMETER FOR B STEEL.

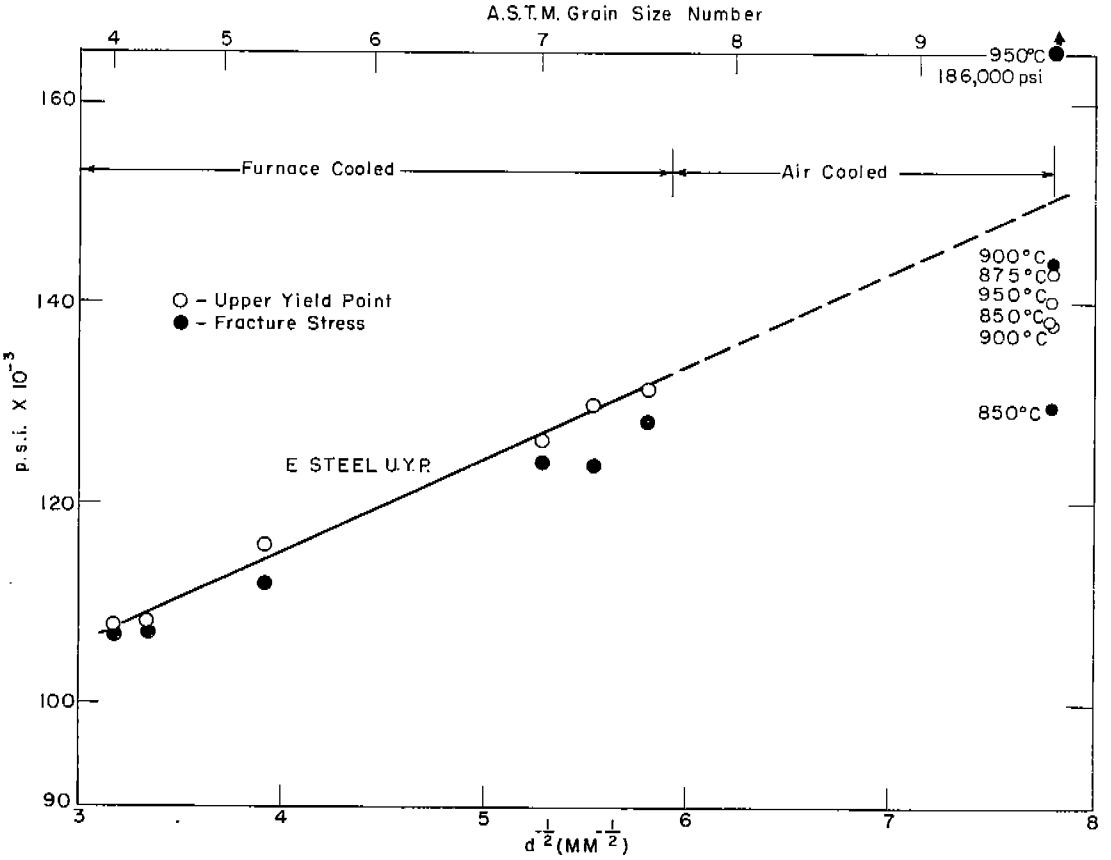

FIG. III. IB-YIELD STRESS AND FRACTURE STRESS AT -195°C AS A FUNCTION OF AVERAGE FERRITE GRAIN DIAMETER FOR E STEEL.

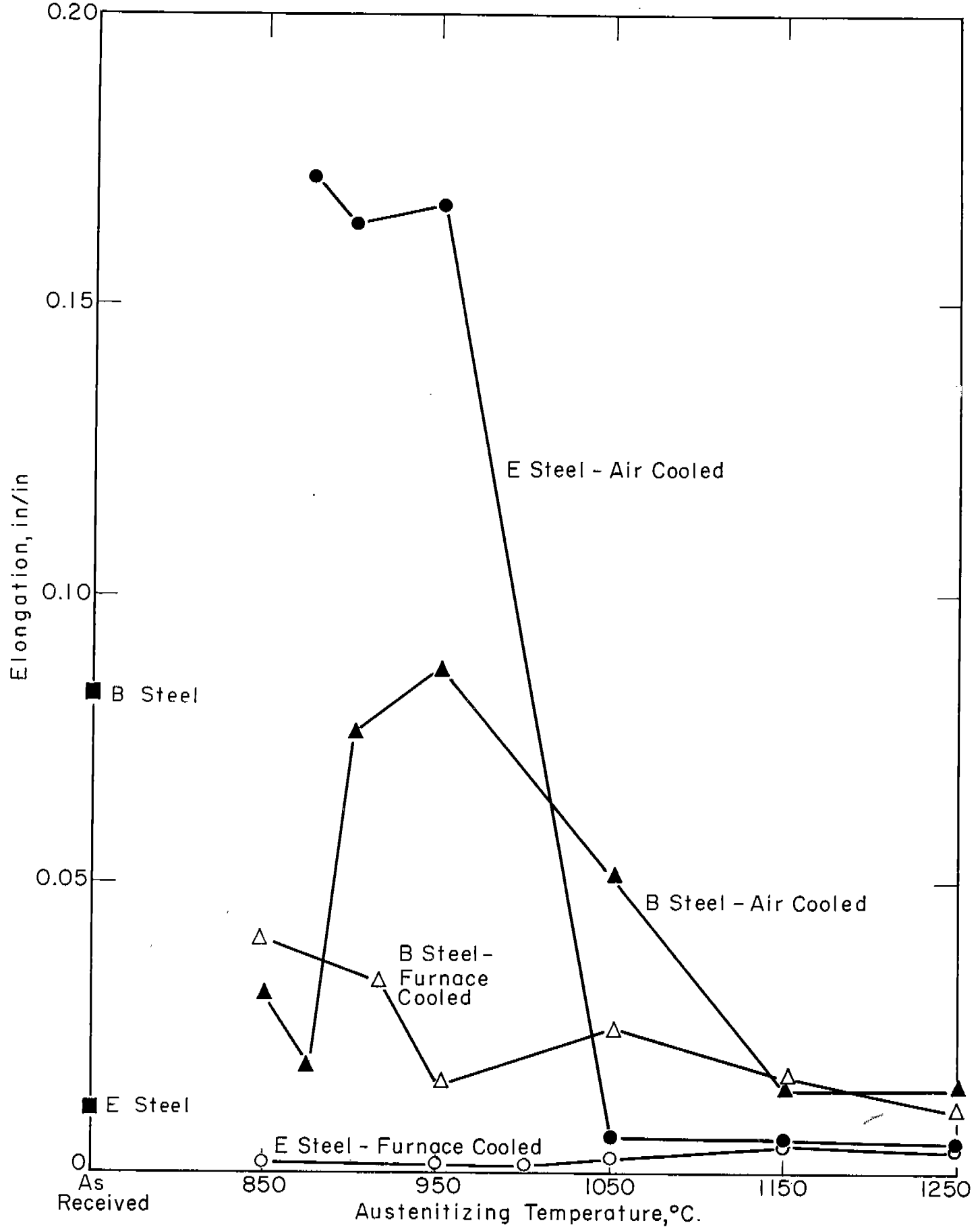

FIG. III.2 — ELONGATION TO FRACTURE AT -195° C.

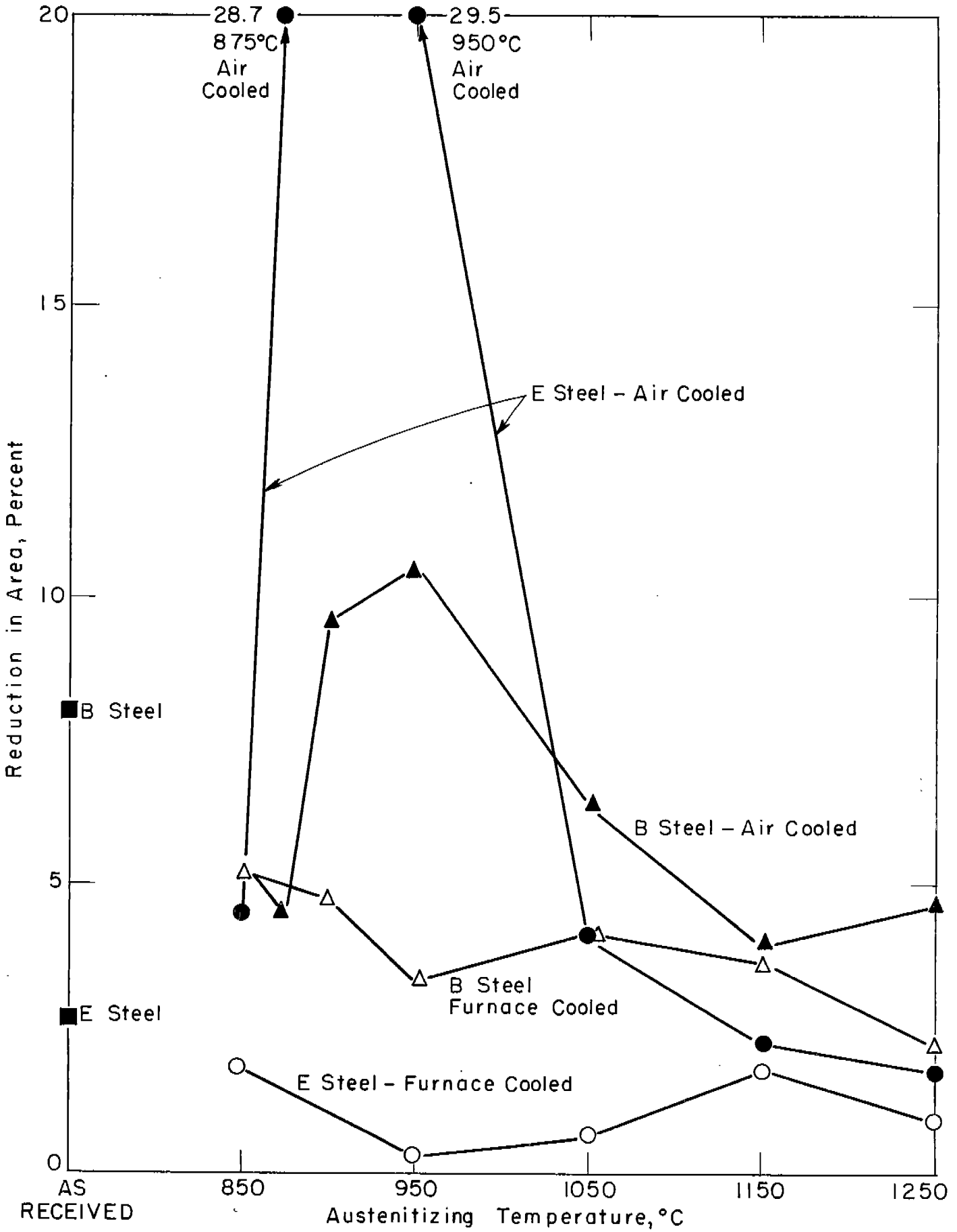

FIG. III 3 - REDUCTION IN AREA AT -195°C.

DISCUSSION OF RESULTS

Provided the ferrite grains were approximately equiaxed, the upper and lower yield stresses were linear functions of $d^{-\frac{1}{2}}$. The relationship was not appreciably affected by changing the cooling rate from furnace to air cooling. As might be expected from the available room temperature data[68], the agreement was better in the case of the lower yield point.

All the specimens with very little ductility had a fracture stress lying between the upper and lower yield stresses. The only logical interpretation of these data appears to be that given by Low[23]; that is, in the completely brittle range the fracture stress lies very close to the yield point. Petch[67] separated the curves by making a correction to the fracture stress. The magnitude of the correction depends upon the amount of ductility preceding fracture and, according to Petch, this decreases as the grain size increases. Within the range being considered, no variation in ductility with grain size was found here. In view of this fact, it is reasonable to conclude that the Petch correlation is unjustified.

Within the brittle range the E steel specimens always broke at a higher stress than those of the B steel of the same grain size. Clearly, the chemistry of the steel is important.

The grain size of the air-cooled specimens of either steel changed by a negligible amount on increasing the austenitizing temperature from 850° C to 950° C. The normalized steels were

more ductile and stronger than the annealed steels. The changes produced by normalizing were more extensive in the case of the E steel. The average fracture stress of E specimens air cooled from 850°, 900°, and 950° C, all with almost identical grain size, was 129, 144, and 186 x 10^3 psi, respectively. These results demonstrate that in ship steel grain size and composition together are insufficient to define the brittle fracture stress. This appears to contradict the work of both Petch and Low, who in the semi-ductile range, found a linear correlation with $d^{-\frac{1}{2}}$. It may be that the discrepancy can be accounted for by the fact that in the earlier work a wide range of grain size was obtained by cold working and heat treatments in which changes in the cooling rate and austenitizing temperature were held to a minimum. Thus, their data showed only a general trend within which considerable variation can be induced by changing the heat treatment used to achieve a particular grain size.

Apart from the present observation that the small-grained (air-cooled) specimens were partly ductile while the larger-grained (furnace-cooled) specimens showed very little ductility, no detailed correlation between ductility and ferrite grain size or any other microstructural parameter was found. This is in line with Brick's observation that when free carbide is present the ductility is no longer a function of grain size. No significant difference was detected in the ductility of annealed specimens of different grain size, but of the same chemistry. Although both series showed

cleavage fractures and small prefracture plastic strain, the B steel had consistently greater ductility than the E in the annealed condition. Over the whole range of heat treatments for steels of the same chemistry the air-cooled specimens had greater ductility than those which were slowly cooled. Those air cooled from between 850° and 950°C showed a particularly marked improvement, the E specimens having even greater ductility than the B specimens. Since all the specimens of one steel had about the same ferrite grain size after air cooling from this range, the sharp increase in ductility with increasing austenitizing temperature cannot be a grain size phenomenon. After air cooling from higher temperatures, the precipitous drop in ductility coincided with the appearance of Widmanstatten structures.

The ductility was measured in two ways: by elongation and by reduction in area. In both cases the scatter in the results from comparable specimens was greater than could be accounted for by experimental errors. This suggests that during the prefracture deformation the initiation of fracture is a chance event. When the probability of the event occurring is large, the ductility and the scatter in the results are small. When the probability is reduced, the ductility and scatter are increased. The reproducibility of experimental ductility data supported this hypothesis.

There is no obvious reason why there should be any direct correlation between the tendency to brittleness as revealed

by the Charpy transition temperature and the quantities measured by the tensile test at -195° C. The Charpy test is concerned with the transition from ductile to brittle behavior, while almost all of the measurements made in the tensile test refer to brittle specimens. Further, the Charpy test measures the behavior of the steel under more complex conditions; the stress is triaxial, the rate of application of the load is rapid, and the temperature is usually greater than -100° C. However, by comparing the results from the two tests and assuming that the Charpy test accurately reflects the resistance of a steel to brittle failure, it is possible to decide which of the simple tensile properties of the material plays the dominant role in determining the brittleness of the steel under practical conditions. It is clear that neither the low-temperature yield stress nor the brittle fracture stress (which shows very little variation with testing temperature[65,66]) is a good measure of the general tendency to brittleness. The fracture and yield stresses of the E steel were consistently higher than the corresponding B specimens of the same grain size or heat treatment. The B steel specimens always had the lower transition temperature.

However, if the specimens are grouped on the basis of chemistry and type of heat treatment, the tensile ductility at -195° C and Charpy 10 ft-lb transition temperature provide approximately the same classification of brittle fracture resistance (compare Figs. II.12 with III.2 or III.3). Both tests

indicated the following ascending order of merit: E steel annealed, E steel normalized 1050--1250° C, B steel annealed, B steel normalized, E steel normalized 850--950° C. The correspondence was not exact, for while the Charpy test showed that normalizing the E steel in the range 850--950° C greatly improved the properties relative to the B steel so that the transition temperatures roughly coincided, the tensile ductility improvement was relatively larger and the E steel displayed a greater ductility than B. Unlike the Charpy transition temperature, the tensile ductility did not have a grain-size dependence within each category. Moreover, the as-received results did not fit unambiguously into this pattern. For the E steel both the transition temperature and the ductility values lay close to those of the furnace-cooled series. However, for the B steel the transition temperature was close to the furnace-cooled and the ductility to the air-cooled series. Thus, although the same general trends are revealed by the two tests, the Charpy test is sensitive to some factors which are not important in determining the low-temperature ductility.

CONCLUSIONS

The following conclusions apply only to ship steel tested at one temperature (-195° C). There is good reason to believe that they cannot be generalized to carbide-free ferrite[1,2]. With this exception, it seems probable that similar results would be

obtained at any temperature in the brittle fracture range. However, it is not known whether or not the characteristics of brittle fracture would remain unaltered at temperatures approaching liquid helium temperature.

1. The upper and lower yield stresses at -195° C are functions of the ferrite grain size provided the grains are approximately equiaxed. The relationship is affected by a change in chemistry but is not influenced appreciably by variations in the cooling rate from the austenitizing temperature.
2. The fracture stress is close to the lower yield stress over the range of treatments which result in brittle behavior. When the ductility is increased, the fracture stress is increased. In a general way the fracture stress increases as the grain size decreases, but this variable is not predominant. In air-cooled specimens compared at the same grain size, the fracture stress increases markedly with the austenitizing temperature in the range of 850°--950° C.
3. The fracture stress (at a given grain size, austenitizing temperature, and cooling rate) is dependent upon the composition of the steel.
4. The ductility appears to be little influenced by ferrite grain size. However, chemistry, cooling rate, and when air cooled, the austenitizing temperature are all influential variables. Air cooling from about 950° C is particularly effective in improving ductility.

5. As judged by comparison with the Charpy test, the ductility before brittle fracture is a more important factor than the fracture stress in determining the susceptibility by brittle behavior.

GENERAL SUMMARY

The major object of this progress report has been to define the quantitative correlations between the microstructure and the tendency toward brittle behavior of two ship steels: a semikilled steel (ABS Class B) and a rimming steel (project steel E). In each series of experiments, a range (850° C to 1300° C) of annealing and normalizing treatments was employed to achieve systematic variations in ferrite-pearlite structures. A study of submicroscopic effects was not included in this part of the program.

Experiments aimed at assessing the role of the conventional microconstituents in the low-temperature deformation and fracture processes are described in Part I. Microexaminations were made on prepolished or sectioned specimens which had been plastically strained (and sometimes fractured) in tension or slow bend (notched or unnotched) tests at room temperature and -195° C. It was found that at -195° C brittle fracture is always preceded by some deformation which is almost entirely the result of slip in ferrite. The slip is heterogeneous on a microscale and appears to be the same as found in room temperature tests. If subcritical Griffith cracks are produced, either they are followed immediately by fracture or, in the specimens used, the number formed is indetectably small.

Twinning, grain boundary effects, or nonmetallic inclusions do not appear to be very significant in the fracture of these ship steels. It was decided that the volume fraction, distribution

and grain size of the ferrite are likely to be the most important microstructural variables, although the influence of pearlite cannot be entirely discounted. The relevant metallographic parameters were measured by lineal analysis with a Hurlbut counter.

In Part II a "staircase" statistical method is described for obtaining an accurate estimate of the 10 ft-lb Charpy V-notch transition temperature using only a moderate number of specimens. In annealed structures, the transition temperature decreases when the ferrite-dependent parameters or pearlite patch size are decreased. For the two ship steels examined, these relationships are strongly linear. However, the mean ferrite path or ferrite grain size is the dominant variable. In a secondary way, the transition temperature increases with the amount of pearlite. The specimens were longitudinal, with the notch perpendicular to the plate surface. With this orientation the effect of pearlite banding is negligible. The transition temperature is lowered by normalizing from 850° C and 950° C, but air cooling from above the latter temperature results in Widmanstatten structures (with microstructural parameters which are insensitive to austenitizing temperature) and higher transition temperature.

Correlations between microstructure (varied by altering the austenitizing temperature) and Charpy transition temperature hold only within a series of tests performed on the same steel with the same cooling rate. The most important conclusion relating to this part of the investigation is that fracture behavior cannot be

predicted in terms of the microstructure alone. Submicroscopic effects produced by alterations in chemistry, cooling rate and, probably austenitizing temperature can be dominant.

In Part III, tensile tests were performed at -195° C on specimens with the same heat treatments as used for the Charpy experiments. The upper and lower yield stresses, fracture stress, elongation and reduction in area at fracture were measured. The upper and lower yield stresses at -195° C are linear functions of the reciprocal square root of the mean ferrite grain diameter ($d^{-\frac{1}{2}}$) provided the grains are approximately equiaxed (i.e., not Widmanstatten). Within the range encountered in the two steels studied, the influence of pearlite on the low temperature tensile properties is negligible. Further, the relationships are not affected by the difference between furnace and air cooling. However, the correlations hold only when the chemistry of the steel is fixed.

The fracture stress as a function of $d^{-\frac{1}{2}}$ is discussed in the light of the mutually incompatible theories of Low and Petch. The results on annealed specimens support Low's view that in the completely brittle range the fracture stress and yield stress are virtually identical. In air-cooled specimens with equiaxed ferrite structure, the fracture stress increases with increase in austenitizing temperature although there is no appreciable change in grain size, a finding which conflicts with the predictions of Petch. Further, it is shown that even in annealed specimens, where the fracture stress does depend on grain size in the expected manner,

the chemistry of the steel enters as a separate variable.

The ductility at -195° C is not markedly influenced by the ferrite grain size. However, the effects of chemistry, cooling rate and, when normalized, the austenitizing temperature are pronounced. A remarkable improvement in ductility is produced by air cooling the steels from within the range 850°--950° C. The project E steel, which in all other conditions has a marked tendency toward brittleness, is particularly responsive to this treatment.

A comparison of the Charpy and low-temperature tensile data reveals no connection between the transition temperature and the brittle fracture stress. However, there is a noteworthy similarity in the general trends of the Charpy transition temperature and the ductility at -195° C with heat treatment. This strongly suggests that both these properties are influenced by many of the same structural conditions. However, the correlation is by no means complete because the low-temperature ductility is not sensitive to the ferrite grain size.

REFERENCES

1. Joseffson, A. Journal of Metals, vol. 6, p. 652, 1954.

2. Smith, R. L., Spangler, G., and Brick, R. M. Trans. A. S. M., vol. 46, p. 973, 1954.

3. Parker, E. R. Brittle Behavior of Engineering Structures. New York: John Wiley & Sons, Inc. (In press).

4. Barrett, C. S., Ansel, G., and Mehl, R. F. Trans. A. S. M. vol. 25, p. 702, 1937.

5. Paxton, H. W., Adams, M., and Massalski, T. B. Phil. Mag., vol. 43, p. 257, 1952.

6. Morton, P. H., Treon, R., and Baldwin, W. M. (Jr.). Jour. of the Mech. and Phys. of Solids, vol. 2, p. 177, 1954.

7. O'Neill, H. Jour. Iron and Steel Inst., vol. 113, p. 417, 1926.

8. Davidenkov, N. N. Izdatel 'stro Akademii Nauk SSSR, vol. 16, 1938.

9. Yakutovich, M. T., and Yakovleva, Y. S. Zhur. Tekh. Fiz., vol. 20, no. 16, 1950.

10. Lifshits, I. M. Zhur. Eksp. i Teort. Fiz., vol. 18, p. 1135, 1948.

11. Bruckner, W. H. "The Micro-Mechanism of Fracture in the Tension-Impact Test," The Welding Journal, Res. Suppl., September 1950, p. 467-s.

12. Bruckner, W. H. Acta Met., vol. 2, p. 168, 1954.

13. Petch, N. J. "The Fracture of Metals," Progress in Metal Physics, vol. 5, no. 1, 1954.

14. Low, J. R. (Jr.), and Feustel, R. G. Acta. Met., vol. 1, p. 185, 1953.

15. Sullivan, P. Sc.M. Thesis, M. I. T., 1955.

16. Geil, G. W., and Carwile, N. L. Trans. A. I. M. E., vol. 197, p. 213, 1953.

17. Allen, N. P. Jour. Iron and Steel Inst., vol. 177, p. 334, 1954.

18. Klier, E. P. Trans. A. S. M., vol. 43, p. 935, 1951.

19. Tipper, C. F., and Sullivan, A. M. Trans. A. S. M., vol. 43, p. 906, 1951.

20. Danko, J. C., and Stout, R. D. "The Effect of Microstructure on the Morphology of Fracture--Part II," paper presented at the national meeting of the American Welding Society, 1955.

21. Griffith, A. A. Phil. Trans. Royal Society, vol. A221, p. 163, 1920.

22. Orowan, E. Fatigue and Fracture of Metals. New York: John Wiley & Sons, Inc., 1952. P. 139.

23. Low, J. R. (Jr.). "Properties and Microstructure," A. S. M. Seminar, 1953, p. 163.

24. Baeyertz, M., Craig, W. F., and Bumps, E. S. Journal of Metals, vol. 185, p. 481, 1949.

25. Felbeck, D. K., and Orowan, E. "Experiments on Brittle Fracture of Steel Plates," The Welding Journal, Res. Suppl., November 1955, p. 570-s.

26. Felix, W. "The Steep Drop in Notch Impact Value of Steel," Doctorate Thesis at the Federal Technical College, Zurich, 1954.

27. Allen, N. P., Rees, W. P., Hopkins, B. E., and Tepler, H. R. Jour. Iron and Steel Inst., vol. 174, p. 108, 1953.

28. Matton-Sjoberg, P., and Lindblom, Y. Jour. Iron and Steel Inst., vol. 177, p. 331, 1954.

29. Rees, W. P., Hopkins, B. E. Jour. Iron and Steel Inst., vol. 172, p. 403, 1952.

30. Hopkins, B. E. Jour. Iron and Steel Inst., vol. 177, p. 332, 1954.

31. Hollomon, J. H. "Fracturing of Metals," A. S. M. Seminar, 1948, p. 262.

32. Barr, W., and Tipper, C. F. Jour. Iron and Steel Inst., vol. 157, p. 223, 1947.

33. Barr, W., and Honeyman, A. J. K. Jour Iron and Steel Inst., vol. 157, pp. 239 and 243, 1947.

34. Gorrissen, J. Jour. Iron and Steel Inst., vol. 162, p. 16, 1949.

35. Rinebolt, J. A., and Harris, W. J. (Jr.). Trans. A. S. M., vol. 43, p. 1175, 1951.

36. Hodge, J. M., Manning, R. D., and Reichhold, H. M. Journal of Metals, vol. 1, p. 233, 1949.

37. Frazier, R. H., Boulger, F. W., and Lorig, C. H. "An Investigation of the Influence of Deoxidation and Chemical Composition on Notched-Bar Properties of Semikilled Ship Steel," Second Progress Report, Ship Structure Committee Report, Serial No. SSC-53, November 28, 1952.

38. Advisory Committee for Project SR-110. "A Review of the Influence of Composition and Deoxidation on the Properties of Ship Plate Steels," Special Report, Ship Structure Committee Report, Serial No. SSC-73, November 16, 1953.

39. Frazier, R. H., Boulger, F. W., and Lorig, C. H. Journal of Metals, vol. 7, p. 323, 1955.

40. Vanderbeck, R. W. "Evaluating Carbon Plate Steels by the Keyhole Charpy Impact Test," The Welding Journal, Res. Suppl., January 1951, pp. 59-s--64-s.

41. Barrett, C. S., and Mahin, W. E. "A Review of Ship Steel Research and Recommendations for Future Studies," Review Report, Ship Structure Committee Report, Serial No. SSC-70, February 15, 1954.

42. Grossman, N. "Pearlitic Structure Effect on Brittle Transition Temperature," The Welding Journal, Res. Suppl., June 1949, pp. 265-s--269-s.

43. Gross, J. H., and Stout, R. D. "The Effect of Microstructure on Notch Toughness--Part I," The Welding Journal, Res. Suppl., October 1951, pp. 481-s--485-s.

44. Rinebolt, J. A. Trans. A. S. M., vol. 46, p. 1527, 1954.

45. Brick, R. M. "Mechanical Properties of High Purity Iron-Carbon Alloys at Low Temperatures," Final Report, Ship Structure Committee Report, Serial No. SSC-94 (To be published).

46. Smith, R. L., Spangler, G., and Brick, R. M. "Effect of Grain Size and Carbon Content on the Low-Temperature Tensile Properties of High Purity Iron-Carbon Alloys," Second Progress Report, Ship Structure Committee Report, Serial No. SSC-81, May 28, 1954.

47. London, G. J., Spangler, G., and Brick, R. M. "Mechanical Properties of High Purity Iron-Carbon Alloys at Low Temperatures," Third Progress Report, Ship Structure Committee Report, Serial No. SSC-93 (To be published).

48. Finney, D. J. "Probit Analysis," Cambridge University Press. 1952.

49. Vanderbeck, R. W., Wilde, R. D., Lindsay, R. W., and Daniel, C. "Statistical Analysis of Behavior in the Transition Temperature Zone," The Welding Journal, Res. Suppl., July 1953, pp. 325-s--332-s.

50. Vanderbeck, R. W., Lindsay, R. W., Wilde, R. D., Lankford, W. T., and Snyder, S. C. "Symposium on Effect of Temperature on the Brittle Behavior of Metals with Particular Reference to Low Temperatures, Special Tech. Publ. No. 158, Philadelphia, A. S. T. M., 1954, p. 308.

51. Ransom, J. T., Mehl, R. F. Trans. A. I. M. E., vol. 185, p. 364, 1949.

52. Ransom, J. T., and Mehl, R. F. A. S. T. M. Special Tech. Publ. No. 137, 1952.

53. Rinebolt, J. A., and Harris, W. J. (Jr.). "Statistical Analysis of Tests of Charpy V-notch and Keyhole Bars," The Welding Journal, Res. Suppl., April 1951, pp. 202-s--208-s.

54. Whitmore, D. H. (Jr.). Sc.D. Thesis, M. I. T., 1955.

55. Howard, R. T., and Cohen, M. Trans. A. I. M. E., vol. 172, p. 413, 1947.

56. Smith, C. S., and Guttman, L. Trans. A. I. M. E., vol. 197, p. 81, 1953.

57. Rutherford, J. J. B., Aborn, R. H., and Bain, H. C. Metals and Alloys, vol. 8, p. 345, 1937.

58. Carpenter, H., Robertson, J. M. Metals, vol. II, Oxford University Press, 1944. P. 831.

59. 1953 Supplement to the Atlas of Isothermal Transformation Diagrams, U. S. Steel Corporation, Pittsburgh, 1953, p. 7.

60. Harris, W. J. (Jr.), Rinebolt, J. A., and Raring, R. "Upper and Lower Transitions in Charpy Test," The Welding Journal, Res. Suppl., September 1951, pp. 417-s--422-s.

61. Petch, N. J. Progress in Metal Physics, London: Pargamon Press, 1954. Vol. 5, p. 52.

62. Noel, P. G. Introduction to Mathematical Statistics, New York: John Wiley & Sons, Inc., 1947.

63. Klier, E. P., and Gensamer, M. "Correlation of Laboratory Tests with Full-Scale Ship Plate Fracture Tests," Final Report, Ship Structure Committee Report, Serial No. SSC-30, January 30, 1953.

64. Klier, E. P., Mack, J. O., Wagner, F. C., and Gensamer, M. "Correlation of Laboratory Tests with Full-Scale Ship Plate Fracture Tests: Analysis of True-Stress True-Strain Data on Project Steels," Progress Report, Ship Structure Committee Report, Serial No. SSC-19, June 21, 1950.

65. Eldin, A. S., and Collins, S. C. Journal of Applied Physics, vol. 22, p. 1296, 1951.

66. Bechtold, J. H. Acta Met., vol. 3, p. 249, 1955.

67. Petch, N. J. Jour. Iron and Steel Inst., vol. 174, p. 25, 1953.

68. Hall, E. O. Proc. Phys. Soc., vol. B64, p. 747, 1951.

69. Allen, N. P. "Symposium on the Mechanical Properties of Metals at Low Temperatures," 1952, U. S. Department of Commerce, National Bureau of Standards Circular 520.

70. Rees, W. P. Jour. Iron and Steel Inst., vol 177, p. 342, 1954 (Discussion to Ref. 67).

71. Cracknell, A., and Petch, N. J. Acta Met, vol. 3, p. 186, 1955.

72. Williams, M. L. "Symposium on Effect of Temperature on the Brittle Behavior of Metals with Particular Reference to Low Temperature," A. S. T. M. 1953.

73. Lement, B. S., Averbach, B. L., and Cohen, M. Trans. A. S. M., vol. 46, p. 851, 1954.